



**T.R.**  
**GEBZE TECHNICAL UNIVERSITY**  
**GRADUATE SCHOOL OF NATURAL AND APPLIED SCIENCES**

**SCATTERING OF A TEM WAVE BY A LARGE  
CIRCUMFERENTIAL GAP ON A HOLLOW AND A  
DIELECTRIC-FILLED COAXIAL WAVEGUIDES**

**HÜLYA ÖZTÜRK**  
**A THESIS SUBMITTED FOR THE DEGREE OF  
DOCTOR OF PHILOSOPHY  
DEPARTMENT OF MATHEMATICS**

**GEBZE**  
**2015**

**T.R.**  
**GEBZE TECHNICAL UNIVERSITY**  
**GRADUATE SCHOOL OF NATURAL AND APPLIED SCIENCES**

**SCATTERING OF A TEM WAVE BY A  
LARGE CIRCUMFERENTIAL GAP ON A  
HOLLOW AND A DIELECTRIC-FILLED  
COAXIAL WAVEGUIDES**

**HÜLYA ÖZTÜRK**  
**A THESIS SUBMITTED FOR THE DEGREE OF  
DOCTOR OF PHILOSOPHY  
DEPARTMENT OF MATHEMATICS**

THESIS SUPERVISOR  
ASSOC. PROF. DR. GÖKHAN ÇINAR

**GEBZE**  
**2015**

**T.C.  
GEBZE TEKNİK ÜNİVERSİTESİ  
FEN BİLİMLERİ ENSTİTÜSÜ**

**TEM DALGALARIN DIŞ DUVARINDA  
SONLU BİR AÇIKLIĞA SAHİP İÇİ BOŞ  
VE DİELEKTRİK MALZEME İLE DOLU  
KOAKSİYEL DALGA KILAVUZLARINDAN  
SAÇILIMI**

**HÜLYA ÖZTÜRK  
DOKTORA TEZİ  
MATEMATİK ANABİLİM DALI**

**DANIŞMANI  
DOÇ. DR. GÖKHAN ÇINAR**

**GEBZE  
2015**

GEBZE TEKNİK ÜNİVERSİTESİ

DOKTORA JÜRİ ONAY FORMU

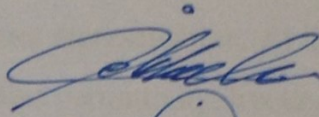
GTÜ Fen Bilimleri Enstitüsü Yönetim Kurulu'nun ..29./..12../2014 tarih ve 2014/..73..... sayılı kararıyla oluşturulan jüri tarafından 09/01/2015 tarihinde tez savunma sınavı yapılan Hülya ÖZTÜRK 'in tez çalışması Matematik Anabilim Dalında DOKTORA tezi olarak kabul edilmiştir.

JÜRİ

ÜYE

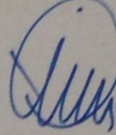
(TEZ DANIŞMANI)

: Doç. Dr. Gökhan ÇINAR



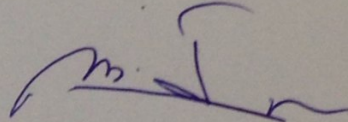
ÜYE

: Prof. Dr. Alinur BÜYÜKAKSOY



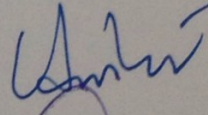
ÜYE

: Prof. Dr. Mansur İSMAİLOV



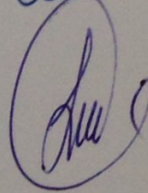
ÜYE

: Doç. Dr. Ahmet DEMİR



ÜYE

: Doç. Dr. İsmail Hakkı TAYYAR



ONAY

Gebze Teknik Üniversitesi Fen Bilimleri Enstitüsü Yönetim Kurulu'nun  
...../...../..... tarih ve ...../..... sayılı kararı.

İMZA/MÜHÜR

## SUMMARY

In this dissertation, the Wiener-Hopf technique has been widely used to analyse the scattering of a TEM wave by a finite gap on the outer wall of a coaxial waveguide. In the first section, it is assumed that inner and outer parts of the waveguide are free space. As for that second geometry, it is investigated that inner part is dielectric-filled while the outer part is free space. By applying the direct Fourier transform to Helmholtz equation, each problem is reduced into the the solution of a modified Wiener-Hopf equation of the first type which is solved via a set of Fredholm integral equations of the second type. Also, with the purpose of point to difficulty of non-conductivity, two different approaches are used for the factorization of the kernel function. Then, numerical results are used to show the excellent agreement between the Wiener-Hopf analysis and simple series representation. At the end of the analysis, the effects of the radii of the walls, relative permittivity, frequency and the gap width on the scattered fields are illustrated graphically.

**Keywords:** Wiener-Hopf method, Electromagnetic wave scattering, Circular waveguide, Circumferential gap, Integral equations.

## ÖZET

Bu çalışmada, koaksiyel dalga kılavuzunun dış duvarındaki sonlu bir açıklığın TEM dalgaların kırınımına etkisi, Wiener-Hopf metodu kullanılarak analiz edilmiştir. İlk bölümde dalga kılavuzunun iç ve dış kısmının boş uzay olduğu durum ele alınmıştır. İkinci bölümde ise içerideki ortamın dielektrik malzeme ile dolu olduğu, dışarıdaki ortamın boş uzay olduğu geometri incelenmiştir. Her bir probleme ilişkin Helmholtz denklemi doğrudan Fourier dönüşümü uygulanması ile birinci tip modifiye Wiener-Hopf denklemlerine indirgenmiş ve bu denklemler ikinci tip Fredholm integral denklemleri aracılığı ile çözülmüştür. Ayrıca, içerideki ortamın dielektrik malzeme ile dolu olmasının ortaya çıkardığı zorluğa dikkat çekmek amacı ile çekirdek fonksiyonunun faktörizasyonunda iki farklı yaklaşım kullanılmıştır. Daha sonra, öncelikli olarak Wiener-Hopf metodu ve Simple Series metodu ile elde edilen sonuçlar grafikler aracılığı ile karşılaştırmalı olarak gösterilmiştir. Buna ilaveten, içerideki ve dışarıdaki silindirlerin yarıçaplarının, dış duvardaki sonlu boşluğun uzunluğunun, frekans değerlerinin ve bağlı dielektrik sabitinin kırınım olayına etkisi incelenmiştir.

**Anahtar Kelimeler:** Wiener-Hopf metodu, Elektromagnetik dalgaların saçılımı , Dairesel dalga kılavuzu, Çevrel boşluk , İntegral denklemler.

## ACKNOWLEDGEMENTS

Foremost, I would like to express my sincere gratitude to my supervisor, Assoc. Prof. Dr. Gökhan ÇINAR, for giving me the opportunity to study with him. Without his incredible support and advice, I would not be able to complete my thesis. His encouragement, motivation and patient guidance has proven to be invaluable to me throughout my time as his student.

Besides, I would like to thank my committee members Prof. Dr. Alinur BÜYÜKAKSOY, Prof. Dr. Mansur İSMAİLOV, Assoc. Prof. Dr. Ahmet DEMİR and Assoc. Prof. Dr. İsmail Hakkı TAYYAR for taking their precious time to consider my work.

A special thanks to my office mates, valuable friends Res. Asst. Fatih KIZILASLAN and Res. Asst. Tuğba YAVUZ for helping me with the numerous questions and making my times more enjoyable that I spent with them.

I'm deeply grateful to my husband Hilmi ÖZTÜRK and my son Efe ÖZTÜRK for making my life meaningful. Thanks to their immeasurable love and support, it has been possible for me to take this work to completion. Finally, I want to thank my dear father, Mahmut ÖZTÜRK for his continued support. I dedicate this thesis to my family.



# TABLE of CONTENTS

	<u>Page</u>
SUMMARY	v
ÖZET	vi
ACKNOWLEDGMENTS	vii
TABLE of CONTENTS	viii
LIST of ABBREVIATIONS and ACRONYMS	ix
LIST of FIGURES	x
1. INTRODUCTION	1
2. SCATTERING OF A TEM WAVE BY A LARGE CIRCUMFERENTIAL GAP ON A COAXIAL WAVEGUIDE	4
2.1. Formulation of the Problem	5
2.2. Analysis of the Fields	15
2.3. Numerical Results	17
3. TEM WAVE RADIATION FROM A DIELECTRIC-FILLED COAXIAL WAVEGUIDE WITH A LARGE CIRCUMFERENTIAL GAP ON ITS OUTER WALL	22
3.1. Formulation of the Problem	22
3.2. Analysis of the Fields	29
3.3. Numerical Results	30
4. CONCLUDING REMARKS	35
REFERENCES	36
BIOGRAPHY	38
APPENDICES	39

## LIST of ABBREVIATIONS and ACRONYMS

### Abbreviations   Explanations and Acronyms

$w$	:	Angular frequency
$\varepsilon_r$	:	Relative permittivity
$\mu_0$	:	Permeability of free space
$\varepsilon_0$	:	Permittivity of free space
$\varepsilon_1$	:	Permittivity of dielectric-filled medium
$k_0$	:	Wave number of free space
$k_1$	:	Wave number of dielectric-filled medium
$l$	:	Length of the gap on outer cylinder
$a$	:	Radius of inner cylinder
$b$	:	Radius of outer cylinder

# LIST of FIGURES

<b><u>Figure No:</u></b>	<b><u>Page</u></b>
2.1: The geometry of the problem.	5
2.2: Complex $\alpha - plane$ .	7
2.3: Geometrical relations for the radiated field.	16
2.4: Comparison of Wiener-Hopf analysis and simple series method.	18
2.5: Radiated field for $a = 0.025$ m, $k_0l = 6$ , $f = 150$ MHz.	19
2.6: Radiated field for $a = 0.025$ m, $b = 2a$ , $f = 150$ MHz.	19
2.7: Radiated field for $a = 0.025$ m, $b = 2a$ , $k_0l = 6$ .	20
2.8: Reflected field for $a = 0.025$ m, $k_0l = 6$ .	20
2.9: Transmitted field for $a = 0.025$ m, $k_0l = 6$ .	21
2.10: Radiated field versus the truncation number N.	21
3.1: Geometry of the problem.	22
3.2: Complex $\alpha - plane$ .	24
3.3: Comparison for $\varepsilon_r = 1$ .	31
3.4: Comparison for $\varepsilon_r = 2.4$ .	32
3.5: Variation of the radiated field with respect to $b/a$ .	32
3.6: Variation of the radiated field with respect to $\varepsilon_r$ .	33
3.7: Variation of the radiated field with respect to frequency.	33
3.8: Variation of the radiated field with respect to $k_1l$ .	34

# 1. INTRODUCTION

The scattering of electromagnetic waves by gaps on the walls of the waveguides has been an important topic in both theory and application, such as microwave bandpass filters, measurement devices, and waveguide radiators. Regarding the need of more accurate modeling of related engineering applications involving electromagnetic wave scattering, the interest in analytical methods has recently increased. [Seran et al., 2009],[Büyükaksoy et al., 2004], [Melkumyan, 2007], [Lee et al., 2011], [Sautbekov, 2011], [Moiola et al., 2011]. [Sheingold and Storer, 1954] analyzed a circular waveguide with a gap on its wall in the case of TE wave incidence by using a variational principle. They found good agreement with experiments for narrow gaps ( small gap width compared to the wavelength ). Later, [Morita and Nakanishi, 1968] investigated the same problem by means of fictitious equivalent magnetic current for the gap. They compared the results with the analysis obtained by Bethe's method and two results agreed well for narrow gaps. [Chang, 1973] studied the coaxial waveguide with a narrow gap in the case of TEM wave incidence, where he formulated an exact integral equation for the aperture field and solved by a quasi-static technique. [Hurd, 1973] also studied the same problem and determined the electric field in a narrow circumferential gap in the outer wall of a coaxial waveguide. [Wait and Hill, 1975a], [Wait and Hill, 1975b] derived field expressions for a dielectric coated coaxial cable with a narrow gap in the shield in the case of TEM wave incidence.

The case where the gap on the wall of a waveguide is large compared to the wavelength is studied by Elmoazzen and Shafai, first for parallel-plate waveguides and TE wave incidence [Elmoazzen and Shafai, 1973], then for circular waveguides and TM wave incidence [Elmoazzen and Shafai, 1974]. They applied direct Fourier transform and reduced the problem into solving a modified Wiener-Hopf technique of the first kind. The resulting Fredholm integral equation of the second type is solved for large gap width compared to the wavelength. The first problem of TE wave propagation in a parallel-plate waveguide with a slit is then studied by [Cho, 1987], where he determined the fields for narrow slits. The second problem of TM wave propagation in circular waveguides with gaps is then analyzed by [Park and Eom, 2003] for thick walls and field expressions are determined by applying a new method based on Fourier

transform and mode-matching techniques.

In this thesis, the TEM wave propagation in a two different coaxial waveguide having a large gap on its outer wall is analysed. In Section 2, it is assumed that the inner and outer parts of the waveguide are free space. In Section 3, as a continuation of the previous section, focused on the case where the interior region of the waveguide is filled with a dielectric material. For each problem, by applying direct Fourier transform, a modified Wiener-Hopf equation of the first type is determined as in [Polat, 1999], [Tayyar et al., 2008], [Çınar and Büyükkaksoy, 2004]. Particularly, when there is a slit/strip type of finite-length scattering mechanisms or discontinuities on the normal direction like steps, modified Wiener-Hopf equations occur. Slit/strips yield a Wiener-Hopf equation in the form of

$$P_-(\alpha) + P_+(\alpha) + G(\alpha)P_1(\alpha) = g(\alpha) \quad (1.1)$$

which involves an entire function unlike classical Wiener-Hopf equations. These are called modified Wiener-Hopf equations of the first type. On the other hand, when there is a step discontinuity, a term with a series appears in the Wiener-Hopf equation to be in the form of

$$G(\alpha)P_-(\alpha) + P_+(\alpha) = g(\alpha) + \sum_{m=0}^{\infty} f_m(\alpha) \quad (1.2)$$

and such equations are called modified Wiener-Hopf equations of the second type. Finally, when there is both slit/strip and step discontinuity, the formulation yields Wiener-Hopf equations involving both an entire function and a series term which are called modified Wiener-Hopf equations of the third type. A more detailed study on modified Wiener-Hopf equations can be found in [Kobayashi, 1993]. Then, the modified Wiener-Hopf equation is reduced to a Fredholm integral equation of the second type, which is solved in a similar fashion as in [Polat, 1999]. Finally, diffraction coefficients related to the reflected, transmitted and radiated fields are determined explicitly. Finally, numerical results are compared with the method described in [Park and Eom, 2003] and the effects of the cross-sectional area of the coaxial cylindrical waveguide and the gap width on the radiated field are presented.

With the analysis done in this thesis, the effect of the relative permittivity of the material inside the waveguide on the method of formulation is clarified, and interestingly, it is found out that when the waveguide is filled with a dielectric material, the factorization method described in [Seran et al., 2009] lacks accuracy. In order to overcome this difficulty, we followed the procedure described in [Mittra and Lee, 1971] and derived new formal expressions for the split functions of the kernel in Appendix C.

Throughout the analysis, a time dependence  $\exp(-i\omega t)$  with  $\omega$  being the angular frequency is assumed.

## 2. SCATTERING OF A TEM WAVE BY A LARGE CIRCUMFERENTIAL GAP ON A COAXIAL WAVEGUIDE

Consider a perfectly conducting coaxial cylindrical waveguide whose inner and outer cylindrical walls are located at  $S = \{\rho = a, -\infty < z < \infty\}$  and  $S = \{\rho = b, (-\infty < z < 0) \cup (l < z < \infty)\}$ , respectively as shown in Figure 2.1. Here, we proposed to study the TEM wave scattering from a large gap on the outer wall rigorously by applying direct Fourier transform which yields a modified Wiener-Hopf equation. Then this modified Wiener-Hopf equation reduced to a pair of simultaneous Fredholm integral equation of the second kind which is solved method of successive approximation. Finally, the diffraction coefficients related to the reflected, transmitted, and radiated fields are determined explicitly. At the end of the analysis, numerical results illustrating the effects of the cross-sectional area of the coaxial cylindrical waveguide and the gap width on the fields are presented as compared with Simple series method.

Let the incident TEM mode propagating in the positive  $z$  direction be given by

$$H_{\phi}^i(\rho, z) = u_i(\rho, z) = \frac{e^{ik_0z}}{\rho} \quad (2.1)$$

where  $k_0$  is the propagation constant which is assumed to have a small imaginary part corresponding to slightly lossy medium. The lossless case can then be obtained by letting  $Im(k_0) \rightarrow 0$  at the end of the analysis. In virtue of the axial symmetry of the problem, all the field components may be expressed in terms of  $H_{\phi}(\rho, z) = u(\rho, z)$  as

$$E_{\rho} = \frac{1}{iw\epsilon_0} \frac{\partial}{\partial z} u(\rho, z), \quad \text{and} \quad E_z = -\frac{1}{iw\epsilon_0} \frac{1}{\rho} \frac{\partial}{\partial \rho} [\rho u(\rho, z)]. \quad (2.2)$$

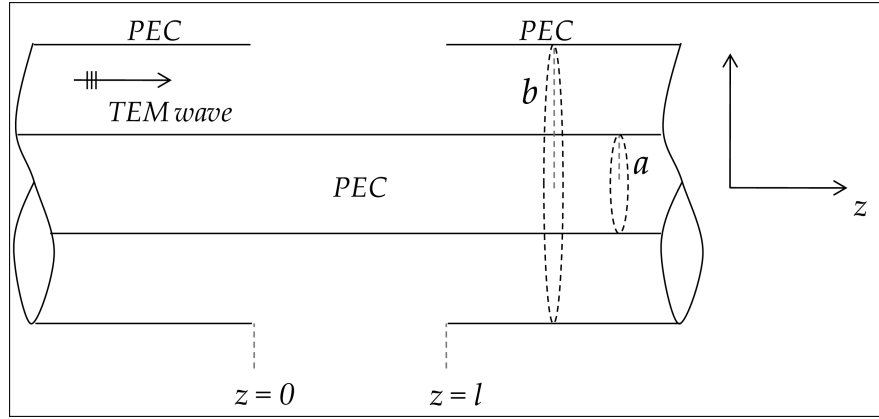


Figure 2.1: The geometry of the problem.

## 2.1. Formulation of the Problem

For the sake of analytical convenience, the total field  $u_T(\rho, z)$  can be expressed as

$$u_T(\rho, z) = \begin{cases} u_i(\rho, z) + u_1(\rho, z) & ; a < \rho < b \\ u_2(\rho, z) & ; \rho > b \end{cases} \quad (2.3)$$

where  $u_1(\rho, z)$  and  $u_2(\rho, z)$  are the scattered fields which satisfy the following differential equation

$$\left[ \frac{\partial^2}{\partial \rho^2} + \frac{1}{\rho} \frac{\partial}{\partial \rho} + \frac{\partial^2}{\partial z^2} + \left( k_0^2 - \frac{1}{\rho^2} \right) \right] u_j(\rho, z) = 0 \quad , \quad j = 1, 2 \quad (2.4)$$

in their domains of validity with the boundary conditions

$$u_1(a, z) + a \frac{\partial}{\partial \rho} u_1(a, z) = 0 \quad , \quad z \in (-\infty, \infty), \quad (2.5)$$

$$u_1(b, z) + b \frac{\partial}{\partial \rho} u_1(b, z) = 0 \quad , \quad z \in (-\infty, 0) \cup (l, \infty), \quad (2.6)$$

$$u_2(b, z) + b \frac{\partial}{\partial \rho} u_2(b, z) = 0 \quad , \quad z \in (-\infty, 0) \cup (l, \infty), \quad (2.7)$$

continuity relations



$$u_1(b, z) + b \frac{\partial}{\partial \rho} u_1(b, z) = u_2(b, z) + b \frac{\partial}{\partial \rho} u_2(b, z) = 0, \quad z \in (0, l), \quad (2.8)$$

$$u_1(b, z) + \frac{e^{ik_0 z}}{b} = u_2(b, z), \quad z \in (0, l). \quad (2.9)$$

Additionally, to ensure the uniqueness of the solution, one has to take into account the radiation condition

$$\frac{\partial u_2}{\partial r} - ik_0 u_2 = O(r^{-1/2}), \quad r = \sqrt{\rho^2 + z^2} \rightarrow \infty, \quad (2.10)$$

and the edge conditions

$$u_T(b, z) = O(1) \quad \text{and} \quad \frac{\partial}{\partial \rho} u_T(b, z) = O(z^{-\frac{1}{3}}), \quad z \rightarrow 0, l. \quad (2.11)$$

The Fourier transform of the Helmholtz equation satisfied by  $u_1(\rho, z)$  with respect to  $z$ , in the range of  $z \in (-\infty, \infty)$  gives

$$\left[ \frac{\partial^2}{\partial \rho^2} + \frac{1}{\rho} \frac{\partial}{\partial \rho} + \left( K_0^2(\alpha) - \frac{1}{\rho^2} \right) \right] F(\rho, \alpha) = 0. \quad (2.12)$$

Here  $K_0(\alpha) = \sqrt{k_0^2 - \alpha^2}$  is the square-root function defined in the complex  $\alpha$ -plane, cut along  $\alpha = k_0$  to  $\alpha = k_0 + i\infty$  and  $\alpha = -k_0$  to  $\alpha = -k_0 - i\infty$ , such that  $K_0(0) = k_0$  as seen in Figure 2.2, and the Fourier transform is defined by

$$F(\rho, \alpha) = F_-(\rho, \alpha) + F_1(\rho, \alpha) + e^{i\alpha l} F_+(\rho, \alpha), \quad (2.13)$$

with

$$F_-(\rho, \alpha) = \int_{-\infty}^0 u_1(\rho, z) e^{i\alpha z} dz, \quad (2.14)$$

$$F_1(\rho, \alpha) = \int_0^l u_1(\rho, z) e^{i\alpha z} dz, \quad (2.15)$$

and

$$F_+(\rho, \alpha) = \int_l^\infty u_1(\rho, z) e^{i\alpha(z-l)} dz. \quad (2.16)$$

Notice that  $F_+(\rho, \alpha)$  and  $F_-(\rho, \alpha)$  are unknown functions which are regular in the

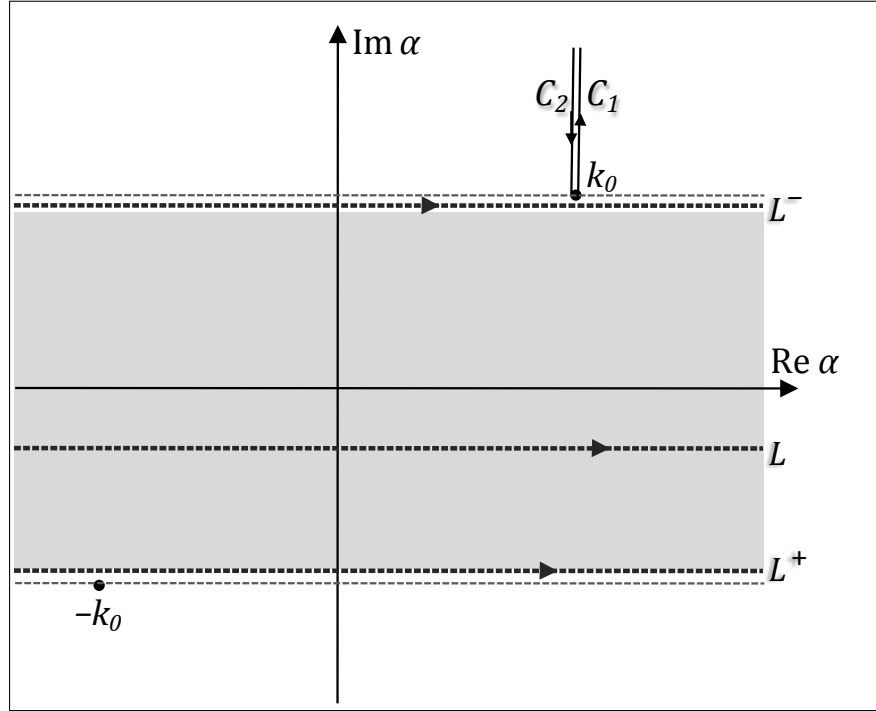


Figure 2.2: Complex  $\alpha$  - plane.

half-planes  $Im(\alpha) > Im(-k_0)$  and  $Im(\alpha) < Im(k_0)$ , respectively, while  $F_1(\rho, \alpha)$  is an entire function of  $\alpha$ . The general solution of equation (2.12) is determined as

$$F(\rho, \alpha) = A(\alpha)J_1(K_0\rho) + B(\alpha)Y_1(K_0\rho), \quad (2.17)$$

where  $A(\alpha)$  and  $B(\alpha)$  are unknown spectral coefficients to be found, and  $J_1(K_0\rho)$  and  $Y_1(K_0\rho)$  are the usual Bessel functions of the first and second kinds, respectively. Applying the Fourier transform of the boundary conditions, (2.5) and (2.6) yields

$$B(\alpha) = -A(\alpha) \frac{J_0(K_0a)}{Y_0(K_0a)}, \quad (2.18)$$

and

$$F_1(b, \alpha) + bF_1'(b, \alpha) = K_0bA(\alpha)J_0(K_0b) + K_0bB(\alpha)Y_0(K_0b), \quad (2.19)$$

to give

$$A(\alpha) = \frac{Y_0(K_0a) [F_1(b, \alpha) + bF_1'(b, \alpha)]}{K_0b [J_0(K_0b)Y_0(K_0a) - J_0(K_0a)Y_0(K_0b)]}. \quad (2.20)$$

In (2.19), the prime denotes the first-degree derivative with respect to  $\rho$ . On the other hand, the Fourier transform of the Helmholtz Equation satisfied by  $u_2(\rho, z)$  with respect to  $z$ , in the range of  $z \in (-\infty, \infty)$  gives

$$\left[ \frac{\partial^2}{\partial \rho^2} + \frac{1}{\rho} \frac{\partial}{\partial \rho} + \left( K_0^2(\alpha) - \frac{1}{\rho^2} \right) \right] G(\rho, \alpha) = 0, \quad (2.21)$$

with

$$G(\rho, \alpha) = G_-(\rho, \alpha) + G_1(\rho, \alpha) + e^{i\alpha l} G_+(\rho, \alpha), \quad (2.22)$$

where  $G_-(\rho, \alpha)$ ,  $G_1(\rho, \alpha)$  and  $G_+(\rho, \alpha)$  are defined similar to that of (2.14) - (2.16) by replacing the function  $u_1(\rho, z)$  with  $u_2(\rho, z)$ .  $G_+(\rho, \alpha)$  and  $G_-(\rho, \alpha)$  are unknown functions which are regular in the half-planes  $Im(\alpha) > Im(-k_0)$  and  $Im(\alpha) < Im(k_0)$ , respectively, while  $G_1(\rho, \alpha)$  is an entire function of  $\alpha$ . The general solution of (2.21) is determined as

$$G(\rho, \alpha) = C(\alpha)H_1^{(1)}(K_0\rho). \quad (2.23)$$

Applying the Fourier transform of the boundary condition (2.7) yields

$$C(\alpha) = \frac{[G_1(b, \alpha) + bG_1'(b, \alpha)]}{K_0bH_0^{(1)}(K_0b)}. \quad (2.24)$$

By taking into account the Fourier transform of the continuity relations (2.8) and (2.9), one gets

$$P_1(\alpha) = G_1(b, \alpha) + bG_1'(b, \alpha) = F_1(b, \alpha) + bF_1'(b, \alpha), \quad (2.25)$$

and

$$F_1(b, \alpha) + \frac{[e^{i(\alpha+k_0)l} - 1]}{ib(\alpha + k_0)} = G_1(b, \alpha), \quad (2.26)$$

respectively, to give

$$\frac{-2}{\pi b^2} \frac{M(\alpha)}{K_0^2(\alpha)} P_1(\alpha) + P_-(\alpha) + e^{i\alpha l} P_+(\alpha) = \frac{e^{i(\alpha+k_0)l}}{ib(\alpha + k_0)} - \frac{1}{ib(\alpha + k_0)}, \quad (2.27)$$

with

$$M(\alpha) = \frac{H_0^{(1)}(K_0 a)}{H_0^{(1)}(K_0 b) [J_0(K_0 b) Y_0(K_0 a) - J_0(K_0 a) Y_0(K_0 b)]}. \quad (2.28)$$

Equation (2.27) is nothing but the modified Wiener-Hopf equation of the first kind to be solved. The first step in solving the modified Wiener-Hopf equation is to factorize the kernel Function  $M(\alpha)$ . This can be done by following the procedures described in [Mittra and Lee, 1971] as

$$M(\alpha) = M_+(\alpha) M_-(\alpha) \quad (2.29)$$

with

$$\begin{aligned} M_+(\alpha) = & \sqrt{M(0)} \prod_{m=1}^{\infty} \frac{1}{(1 + \alpha/\delta_m) e^{i\alpha(b-a)/m\pi}} \\ & \times \exp \left[ \frac{ik(b-a)}{2} + \frac{K(\alpha)(a-b)}{\pi} \log \frac{\alpha + iK(\alpha)}{k} + q(\alpha, a) - q(\alpha, b) \right] \\ & \times \exp \left\{ \frac{\alpha}{\pi i} (b-a) \left[ 1 - C + \log \left( \frac{2\pi i}{k(b-a)} \right) \right] \right\}, \end{aligned} \quad (2.30)$$

and

$$M_-(\alpha) = M_+(-\alpha). \quad (2.31)$$

In (2.30),  $C$  is the Euler's constant given by  $C = 0.57721566\dots$  and  $q(\alpha, \rho_1)$  is the integral

$$q(\alpha, \rho_1) = \frac{1}{\pi} P \int_0^{\infty} \left[ 1 - \frac{2}{\pi x} \frac{1}{J_0^2(x) + Y_0^2(x)} \right] \log \left( 1 + \frac{\alpha \rho_1}{[(k_0 \rho_1)^2 - x^2]^{1/2}} \right) dx \quad (2.32)$$

Above, the letter  $P$  denotes the Cauchy principle value at the singularity  $x = k_0 \rho_1$ . By standard asymptotics, we have  $M_{\pm}(\alpha) = O(\pm \alpha^{-1/2})$  as  $|\alpha| \rightarrow \infty$ . In the split function  $M_+(\alpha)$ , the poles of  $M(\alpha)$  are  $\delta_m$ 's satisfying  $\delta_m = \sqrt{k_0^2 - \xi_m^2}$ ,  $m = 1, 2, \dots$  with

$$J_0(\xi_m b) Y_0(\xi_m a) - J_0(\xi_m a) Y_0(\xi_m b) = 0, \quad m = 1, 2, \dots \quad (2.33)$$

Now, multiplying all terms of (2.27) by  $(k_0 + \alpha) e^{-i\alpha l} / M_+(\alpha)$ , one gets

$$-\frac{2}{\pi b^2} \frac{M_-(\alpha)}{(k_0 - \alpha)} P_1(\alpha) e^{-i\alpha l} + e^{-i\alpha l} \frac{(k_0 + \alpha)}{M_+(\alpha)} L(\alpha) + \frac{(k_0 + \alpha)}{M_+(\alpha)} U(\alpha) = 0 \quad (2.34)$$

with

$$U(\alpha) = P_+(\alpha) - \frac{e^{ik_0 l}}{ib(\alpha + k_0)} \quad (2.35)$$

and

$$L(\alpha) = P_-(\alpha) + \frac{1}{ib(\alpha + k_0)}. \quad (2.36)$$

Obviously, in (2.34), the first and third terms are regular in the lower and upper half-planes, respectively. However, the second term has singularities in both half-planes. Because of this, it is compulsory to apply the Wiener-Hopf decomposition as

$$\begin{aligned} & e^{-i\alpha l} \frac{(k_0 + \alpha)}{M_+(\alpha)} L(\alpha) \\ &= \frac{1}{2\pi i} \int_{L^+} e^{-i\tau l} \frac{(k_0 + \tau)}{M_+(\tau)} \frac{L(\tau)}{(\tau - \alpha)} d\tau - \frac{1}{2\pi i} \int_{L^-} e^{-i\tau l} \frac{(k_0 + \tau)}{M_+(\tau)} \frac{L(\tau)}{(\tau - \alpha)} d\tau \end{aligned} \quad (2.37)$$

Hence, (2.34) can be rearranged as

$$\begin{aligned} \frac{2M_-(\alpha) P_1(\alpha) e^{-i\alpha l}}{\pi b^2 (k_0 - \alpha)} + \frac{1}{2\pi i} \int_{L^-} \frac{e^{-i\tau l} (k_0 + \tau) L(\tau)}{M_+(\tau) (\tau - \alpha)} d\tau \\ = \frac{1}{2\pi i} \int_{L^+} \frac{e^{-i\tau l} (k_0 + \tau) L(\tau)}{M_+(\tau) (\tau - \alpha)} d\tau + \frac{(k_0 + \alpha) U(\alpha)}{M_+(\alpha)} \end{aligned} \quad (2.38)$$

While the left hand side of the above equation is regular in the lower half-plane, right hand side of the same equation is regular in the upper half-plane. By performing analytical continuation principle together with the Liouville' theorem yields

$$\frac{(k_0 + \alpha) U(\alpha)}{M_+(\alpha)} = -\frac{1}{2\pi i} \int_{L^+} e^{-i\tau l} \frac{(k_0 + \tau) L(\tau)}{M_+(\tau) (\tau - \alpha)} d\tau \quad (2.39)$$

On the other hand, multiplying all terms of (2.27) by  $(k_0 - \alpha) / M_-(\alpha)$ , we get

$$\begin{aligned} -\frac{2}{\pi b^2} \frac{M_+(\alpha)}{(k_0 + \alpha)} P_1(\alpha) + \frac{(k_0 - \alpha)}{M_-(\alpha)} P_-(\alpha) + e^{i\alpha l} \frac{(k_0 - \alpha)}{M_-(\alpha)} U(\alpha) \\ = -\frac{1}{ib(k_0 + \alpha)} \frac{(k_0 - \alpha)}{M_-(\alpha)} \end{aligned} \quad (2.40)$$

Similar to the upper case, one has necessarily to apply decomposition for the third term and the right hand side of (2.40) as

$$\begin{aligned} e^{i\alpha l} \frac{(k_0 - \alpha)}{M_-(\alpha)} U(\alpha) \\ = \frac{1}{2\pi i} \int_{L^+} e^{i\tau l} \frac{(k_0 - \tau) U(\tau)}{M_-(\tau) (\tau - \alpha)} d\tau - \frac{1}{2\pi i} \int_{L^-} e^{i\tau l} \frac{(k_0 - \tau) U(\tau)}{M_-(\tau) (\tau - \alpha)} d\tau \end{aligned} \quad (2.41)$$

and

$$-\frac{1}{ib(k_0 + \alpha)} \frac{(k_0 - \alpha)}{M_-(\alpha)} = f_+(\alpha) \mp f_-(\alpha) \quad (2.42)$$

with

$$\begin{aligned}
f_+(\alpha) &= \frac{1}{2\pi i} \int_{L^+} -\frac{1}{ib(k_0 + \tau)} \frac{(k_0 - \tau)}{M_-(\tau)(\tau - \alpha)} d\tau, \\
&= \frac{1}{2\pi i} \left\{ -2\pi i \times \text{Rez} \left( -\frac{1}{ib(k_0 + \tau)} \frac{(k_0 - \tau)}{M_-(\tau)(\tau - \alpha)}, -k_0 \right) \right\}, \\
&= -\frac{2k_0}{ibM_+(k_0)(k_0 + \alpha)}.
\end{aligned} \tag{2.43}$$

and

$$f_{-\alpha} = -\frac{1}{ib(k_0 + \alpha)} \left[ \frac{(k_0 - \alpha)}{M_-(\alpha)} - \frac{2k_0}{M_+(k_0)} \right]. \tag{2.44}$$

If we substitute these result in (2.40) and apply the analytical continuation principle again, one obtains

$$\frac{(k_0 - \alpha)}{M_-(\alpha)} L(\alpha) = \frac{1}{2\pi i} \int_{L^-} e^{i\tau l} \frac{(k_0 - \tau)}{M_-(\tau)} \frac{U(\tau)}{(\tau - \alpha)} d\tau + \frac{2k_0}{ib(k_0 + \alpha)} \frac{1}{M_+(k_0)}. \tag{2.45}$$

(2.39) and (2.45) are Fredholm integral equations of the second type to be solved. The paths of integration  $L^+$  nad  $L^-$  in these integral equations are depicted in Figure 2.2. Changing the integration variable  $\tau$  by  $-\tau$  in (2.39) and replacing  $\alpha$  by  $-\alpha$  in (2.45), the addition and subtraction of the resulting equations yield

$$\frac{(k_0 + \alpha)}{M_+(\alpha)} \tilde{U}(\alpha) = \frac{1}{2\pi i} \int_{L^-} e^{i\tau l} \frac{(k_0 - \tau)}{M_-(\tau)} \tilde{U}(\tau) \frac{d\tau}{(\tau + \alpha)} + \frac{2k_0}{ib(k_0 - \alpha)} \frac{1}{M_+(k_0)} \tag{2.46}$$

and

$$\frac{(k_0 + \alpha)}{M_+(\alpha)} \tilde{L}(\alpha) = -\frac{1}{2\pi i} \int_{L^-} e^{i\tau l} \frac{(k_0 - \tau)}{M_-(\tau)} \tilde{L}(\tau) \frac{d\tau}{(\tau + \alpha)} - \frac{2k_0}{ib(k_0 - \alpha)} \frac{1}{M_+(k_0)} \tag{2.47}$$

respectively, where  $\tilde{U}(\alpha)$  and  $\tilde{L}(\alpha)$  are defined by

$$\tilde{U}(\alpha) = U(\alpha) + L(-\alpha) \tag{2.48}$$

and

$$\tilde{L}(\alpha) = U(\alpha) - L(-\alpha). \quad (2.49)$$

Hence, the problem is reduced to the solution of two integral equations (2.46) and (2.47) which can be solved by using an iterative procedure that produces a Neumann series expansion of solutions. The asymptotical analysis of this type of integrals has been done in detail in [Serbest and Büyükaksoy, 1993] where it is proved that an iterative solution is possible when  $k_0 l \gg 1$ . Following the procedure described in [Serbest and Büyükaksoy, 1993] for large  $k_0 l$ , it is found that the first terms lying in the right-hand sides of equations (2.46) and (2.47) give the first-order solution. Second-order solutions can then be obtained by replacing the unknown functions appearing in the integrands by their first-order approximations. Higher-order terms can be obtained by following the same procedure to give  $\tilde{U}(\alpha) = \tilde{U}^{(1)}(\alpha) + \tilde{U}^{(2)}(\alpha) + \tilde{U}^{(3)}(\alpha) + \dots$  and  $\tilde{L}(\alpha) = \tilde{L}^{(1)}(\alpha) + \tilde{L}^{(2)}(\alpha) + \tilde{L}^{(3)}(\alpha) + \dots$ . Then, the first-order solutions are determined to be

$$\tilde{U}^{(1)}(\alpha) = -\tilde{L}^{(1)}(\alpha) = \frac{2k_0}{ib(k_0 - \alpha)} \frac{1}{M_+(k_0)} \frac{M_+(\alpha)}{(k_0 + \alpha)} \quad (2.50)$$

while the second-order solutions become

$$\begin{aligned} \tilde{U}^{(2)}(\alpha) &= \frac{M_+(\alpha)}{(k_0 + \alpha)} \frac{1}{2\pi i} \int_{L^-} e^{i\tau l} \frac{1}{M_-(\tau)} \left[ \frac{2k_0}{ib(k_0 + \tau)} \frac{M_+(\tau)}{M_+(k_0)} \right] \frac{d\tau}{(\tau + \alpha)}, \\ &= -\frac{k_0}{b\pi} \frac{M_+(\alpha)}{(k_0 + \alpha) M_+(k_0)} I_1(\alpha). \end{aligned} \quad (2.51)$$

and

$$\begin{aligned} \tilde{L}^{(2)}(\alpha) &= \frac{M_+(\alpha)}{(k_0 + \alpha)} - \frac{1}{2\pi i} \int_{L^-} e^{i\tau l} \frac{1}{M_-(\tau)} \left[ -\frac{2k_0}{ib(k_0 + \tau)} \frac{M_+(\tau)}{M_+(k_0)} \right] \frac{d\tau}{(\tau + \alpha)}, \\ &= -\frac{k_0}{b\pi} \frac{M_+(\alpha)}{(k_0 + \alpha) M_+(k_0)} I_1(\alpha). \end{aligned} \quad (2.52)$$

with



$$I_1(\alpha) = \int_{L^-} e^{i\tau l} \frac{[M_+(\tau)]^2}{M(\tau)} \frac{1}{(k_0 + \tau)(\tau + \alpha)} d\tau. \quad (2.53)$$

By virtue of Jordan's lemma,  $L^-$  can be deformed to the branch-cut integral along  $C_1$  and  $C_2$  as

$$I_1(\alpha) = \int_{C_1-C_2} e^{i\tau l} \frac{[M_+(\tau)]^2}{M(\tau)} \frac{1}{(k_0 + \tau)(\tau + \alpha)} d\tau \quad (2.54)$$

Using properties  $J_0(-K_0b) = J_0(K_0b)$ ,  $Y_0(-K_0a) = Y_0(K_0a) + 2iJ_0(K_0a)$ ,  $H_0^{(1)}(-K_0a) = -J_0(K_0a) + iY_0(K_0a)$  and making the substitution  $k_0 - \tau = te^{-i\pi/2}$ ,  $t > 0$ , the above integrals can be reduced to

$$\begin{aligned} I_1(\alpha) &= \int_{C_1-C_2} e^{i\tau l} \frac{[M_+(\tau)]^2}{(k_0 + \tau)(\tau + \alpha)} \frac{1}{M(\tau)} d\tau, \\ &= \int_0^\infty \frac{e^{i(k_0+it)l} [M_+(k_0+it)]^2 2 [J_0(K_0b)Y_0(K_0a) - J_0(K_0a)Y_0(K_0b)]^2}{(2ik_0 - t)(k_0 + it + \alpha) [J_0^2(K_0a) + Y_0^2(K_0a)]} dt, \quad (2.55) \\ &= \frac{e^{ik_0l} [M_+(k_0)]^2}{ik_0} \beta(a, b, l; \alpha). \end{aligned}$$

with

$$\beta(a, b, l; \alpha) = \int_0^\infty \frac{e^{-tl}}{[t - i(k_0 + \alpha)]} \frac{[J_0(K_0b)Y_0(K_0a) - J_0(K_0a)Y_0(K_0b)]^2}{J_0^2(K_0a) + Y_0^2(K_0a)} dt \quad (2.56)$$

is to be evaluated numerically. Above,  $K_0 = \sqrt{t^2 - 2ikt}$ . Finally, the solution of the modified Wiener-Hopf equation reads

$$P_1(\alpha) = -\frac{i\pi k_0 b}{M_+(k_0)M_+(\alpha)} + \frac{ib e^{i(\alpha+k_0)l} (k_0 - \alpha) M_+(k_0)}{2 M_-(\alpha)} \beta(a, b, l; \alpha). \quad (2.57)$$

## 2.2. Analysis of the Fields

The radiated field in the region  $\rho > b$ ,  $-\infty < z < \infty$ , namely,  $u_2(\rho, z)$  can be solved by the below inverse Fourier transform integral

$$u_2(\rho, z) = \frac{1}{2\pi} \int_L P_1(\alpha) \frac{H_1^{(1)}(K_0\rho)}{K_0 b H_0^{(1)}(K_0 b)} e^{-i\alpha z} d\alpha, \quad (2.58)$$

where  $L$  is the line depicted in Figure 2.2, lying in the strip  $Im(-k_0) < Im(\alpha) < Im(k_0)$ . Utilizing the asymptotic expansion of  $H_1^{(1)}(K_0\rho) \rightarrow \sqrt{\frac{2}{\pi K_0\rho}} e^{i(K_0\rho - 3\pi/4)}$  as  $\rho \rightarrow \infty$ , the asymptotic evaluation of the above integral, using the saddle point technique, yields

$$u_2(r, \theta) = D(\theta) \frac{e^{ik_0 r}}{k_0 r} \quad (2.59)$$

with

$$D(\theta) = \frac{ik_0}{H_0^{(1)}(k_0 b \sin \theta) \sin \theta} \left\{ \frac{1}{M_+(k_0) M_-(k_0 \cos \theta)} - \frac{e^{ik_0 l(1-\cos \theta)} (1 + \cos \theta) M_+(k_0)}{2\pi M_+(k_0 \cos \theta)} \beta(a, b, l, -k_0 \cos \theta) \right\}. \quad (2.60)$$

Here,  $r$  and  $\theta$  are the spherical coordinates defined by  $\rho = r \sin \theta$  and  $z = r \cos \theta$ , which are presented in Figure 2.3. On the other hand, the diffracted field in the region  $a < \rho < b$ ,  $-\infty < z < \infty$  can be determined by the integral

$$u_1(\rho, z) = \frac{1}{2\pi} \int_L \frac{P_1(\alpha) [J_1(K_0\rho) Y_0(K_0 a) - J_0(K_0 a) Y_1(K_0\rho)]}{K_0 b [J_0(K_0 b) Y_0(K_0 a) - J_0(K_0 a) Y_0(K_0 b)]} e^{-i\alpha z} d\alpha. \quad (2.61)$$

In order to determine the reflected field, the above integral must be evaluated for  $z < 0$ . Taking into account the asymptotic behaviour of  $M_+(\alpha)$ , (2.61), and the standard asymptotics related to the Bessel functions of the first and second type, one can show that the integrand in (2.61) tends to zero for  $|\alpha| \rightarrow \infty$ . This allows the application

of the Jordan's lemma and by virtue of Jordan's lemma and the application of the law residues, the above integral becomes equal to the sum of the residues related to the poles occuring at the simple zeros of  $K_0^2 [J_0(K_0b) Y_0(K_0a) - J_0(K_0a) Y_0(K_0b)]$  lying in the upper half-plane, namely, at  $\alpha = k_0$  and  $\alpha = \alpha'_m$ s. Defining the reflected field in this region as

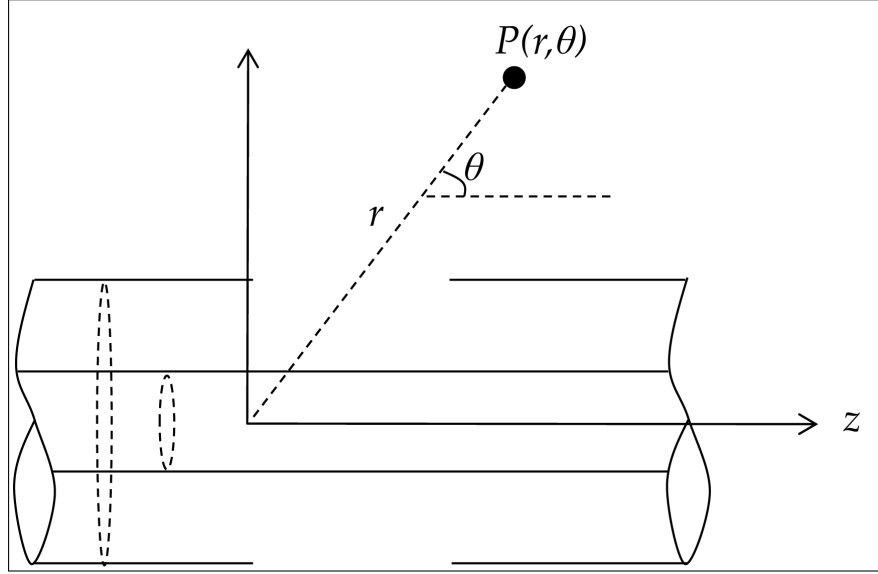


Figure 2.3: Geometrical relations for the radiated field.

$$u_1(\rho, z) = R_0 \frac{e^{-ik_0z}}{\rho} + \sum_{m=1}^{\infty} R_m \psi_m(\rho) e^{-i\alpha_m z}, \quad a < \rho < b, \quad z < 0 \quad (2.62)$$

with

$$\psi_m(\rho) = \frac{\pi}{2} K_m [J_1(K_m \rho) Y_0(K_m a) - J_0(K_m a) Y_1(K_m \rho)], \quad (2.63)$$

one gets

$$R_0 = -\frac{\pi}{2 \log(a/b)} \frac{1}{[M_+(k_0)]^2} \quad (2.64)$$

and

$$R_m = \frac{2k_0}{M_+(k_0) M_+(\alpha_m)} \frac{1}{\{K_0^2 [J_0(K_0b) Y_0(K_0a) - J_0(K_0a) Y_0(K_0b)]\}'_{\alpha \rightarrow \alpha_m}} \quad (2.65)$$

Here,  $R_0$  corresponds to the reflection coefficient for the fundamental TEM mode. Similarly, defining the field in the region  $a < \rho < b, z > l$  as

$$u_1(\rho, z) = -\frac{e^{ik_0z}}{\rho} + T_0 \frac{e^{ik_0z}}{\rho} + \sum_{m=1}^{\infty} T_m \psi_m(\rho) e^{i\alpha_m z}, \quad a < \rho < b, z > l \quad (2.66)$$

and evaluating the integral (2.61) in a similar fashion, the transmission coefficients are found as

$$T_0 = \frac{\beta(a, b, l, -k_0)}{2 \log(a/b)} \quad (2.67)$$

and

$$T_m = \frac{1}{\pi} \frac{e^{i(k_0 - \alpha_m)l} (k_0 + \alpha_m) M_+(k_0)}{M_+(\alpha_m)} \beta(a, b, l, -\alpha_m) \times \frac{1}{\{K_0^2 [J_0(K_0 b) Y_0(K_0 a) - J_0(K_0 a) Y_0(K_0 b)]\}'_{\alpha \rightarrow -\alpha_m}}. \quad (2.68)$$

## 2.3. Numerical Results

For the radiated, reflected, and transmitted fields, some numerical results are obtained and are shown in Figures 2.4-2.10. The infinite integrals in (2.32) and (2.56) are evaluated numerically. In Figure 2.4, the results obtained in this analysis are compared to a previous study by [Park and Eom, 2000], where they analyzed TM wave propagation along an N-slot coaxial line with thick outer wall by applying the simple series method. In order to make such a comparison available, the wall thickness is assumed to be zero and the results are used for the limiting case of one slot only. Figure 2.4 shows that the simple series method in [Park and Eom, 2000] and the Wiener-Hopf analysis in this paper have an excellent agreement. In Figures 2.5-2.7, the variation of the radiated field pattern, normalized as  $|D(\theta)| / |1/a|$  with respect to the observation angle  $\theta$  is presented for different values of  $b/a, k_0 l$ , and frequency. In these figures, strong radiation is observed in the forward and backward directions along the waveguide walls, due to the directive effect of the outer surface of the waveguide walls

for TEM waves. This characteristic is also seen in the case of a circular waveguide with a large gap on its wall, which is studied rigorously in [Elmoazzen and Shafai, 1974]. In Figure 2.5, it can be observed that the magnitude of the radiated field increases with  $b/a$  ratio, which means for a larger cross-sectional area in the coaxial waveguide, more energy will be radiated to the outer space. On the other hand, very little dependence to  $k_0l$  is observed for the observation angles  $\theta < 60^\circ$ , as shown in Figure 2.6, while the radiated field seems to be almost totally insensitive to  $k_0l$  for  $\theta > 100^\circ$ . When the frequency is increased, the magnitude of the radiated field also increases as it is observed in Figure 2.7. This is expected as decreasing the wavelength or increasing the cross-sectional area of the waveguide should have a similar effect. The dependences of the reflection and transmission coefficients of the fundamental TEM mode to the cross-sectional area of the waveguide are also investigated as seen in Figures 2.8 and 2.9. The frequency range in these figures is 100 MHz-2.5 GHz where there is still only TEM mode propagating. As expected, when  $b/a$  ratio increases,  $|R_0|$  decreases, while  $|T_0|$  increases. Figure 2.10 shows the magnitude of the radiated field versus the truncation number ( $N$ ) for different values of  $b/a$ . It can be seen that radiated field amplitude becomes insensitive to the increase of the truncation number for  $N > 4$ .

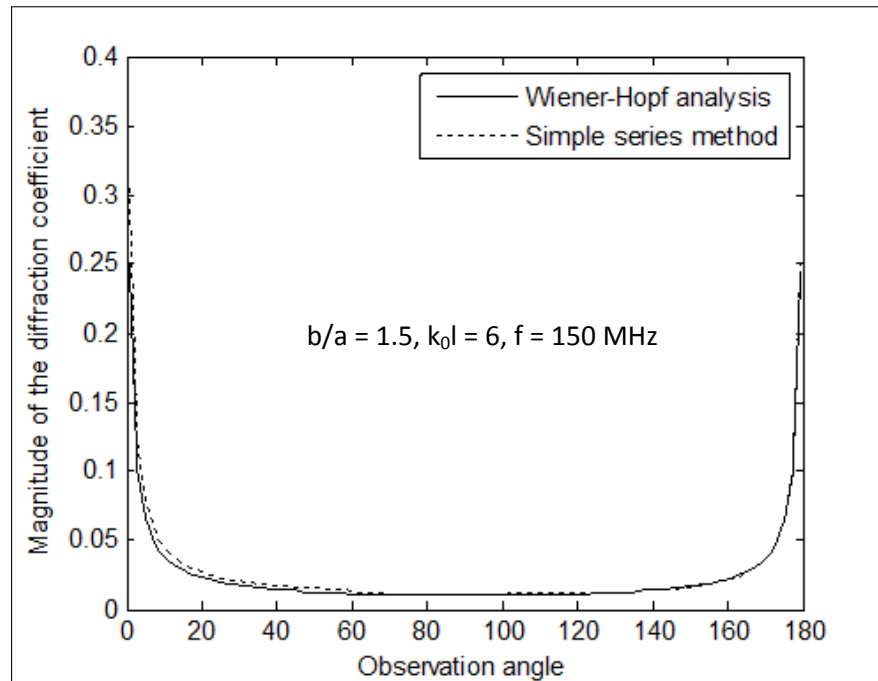


Figure 2.4: Comparison of Wiener-Hopf analysis and simple series method.

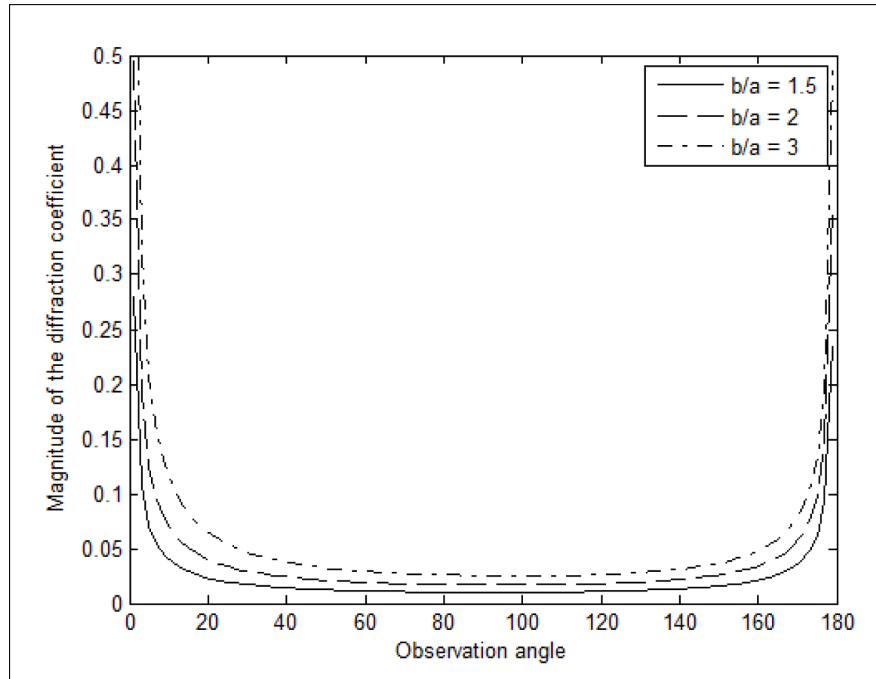


Figure 2.5: Radiated field for  $a = 0.025$  m,  $k_0 l = 6$ ,  $f = 150$  MHz.

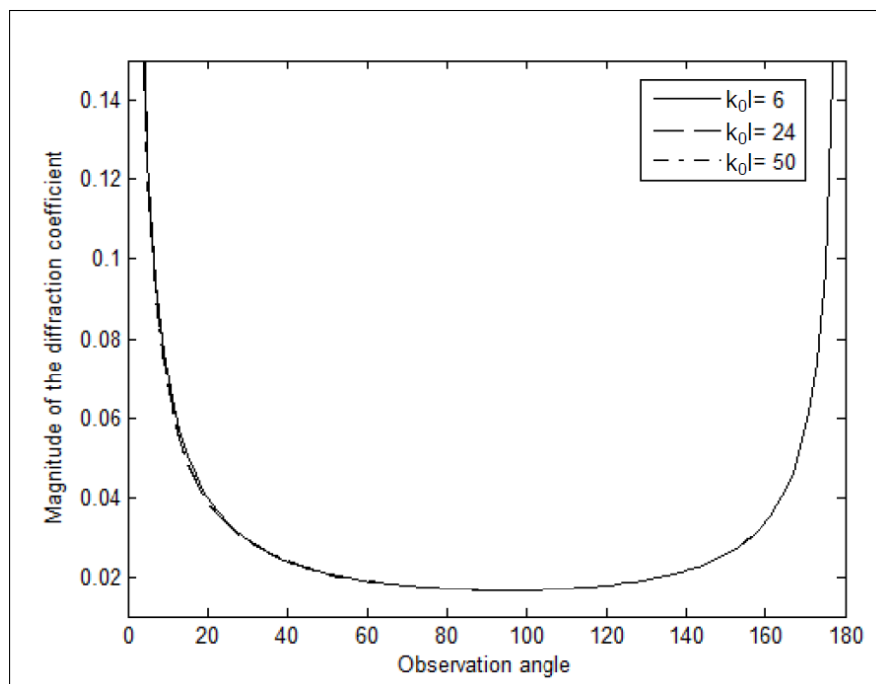


Figure 2.6: Radiated field for  $a = 0.025$  m,  $b = 2a$ ,  $f = 150$  MHz.

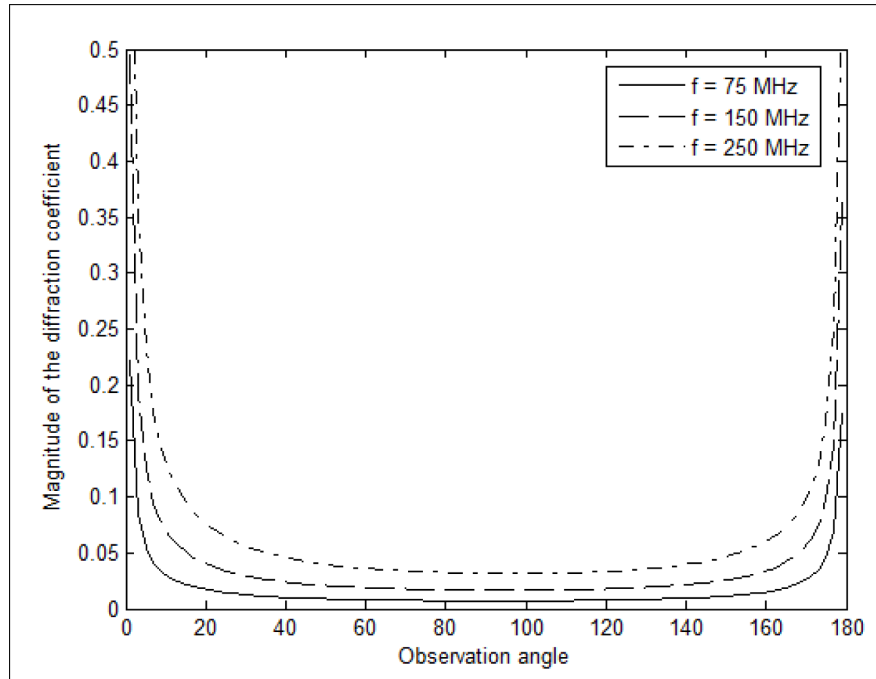


Figure 2.7: Radiated field for  $a = 0.025$  m,  $b = 2a$ ,  $k_0l = 6$ .

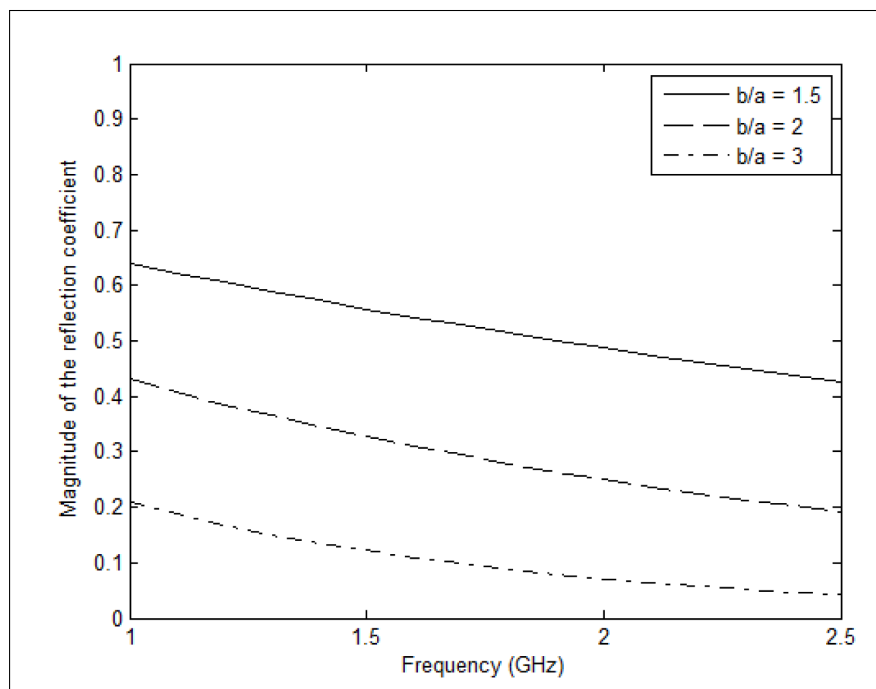


Figure 2.8: Reflected field for  $a = 0.025$  m,  $k_0l = 6$ .

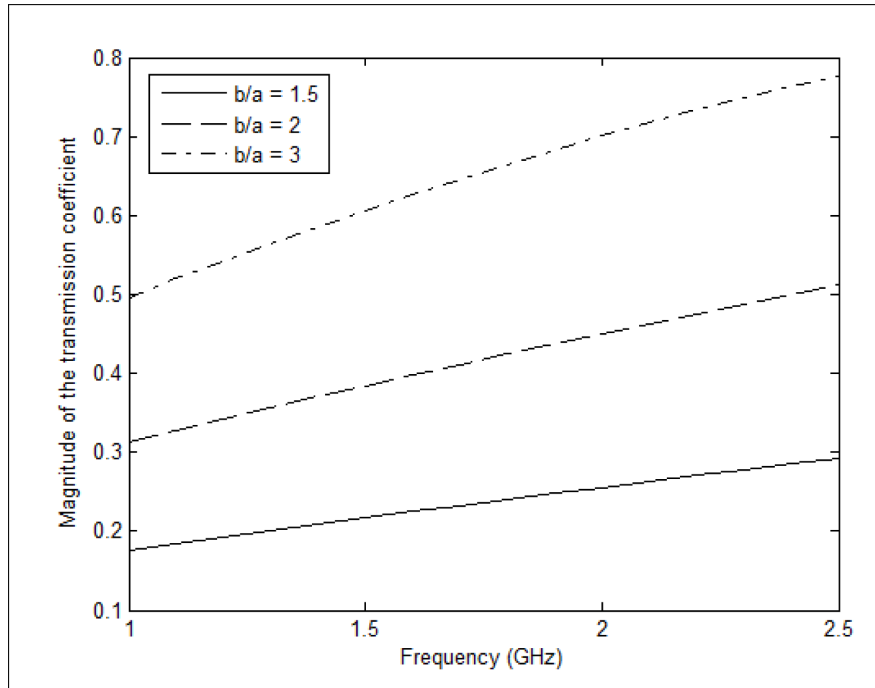


Figure 2.9: Transmitted field for  $a = 0.025$  m,  $k_0 l = 6$ .

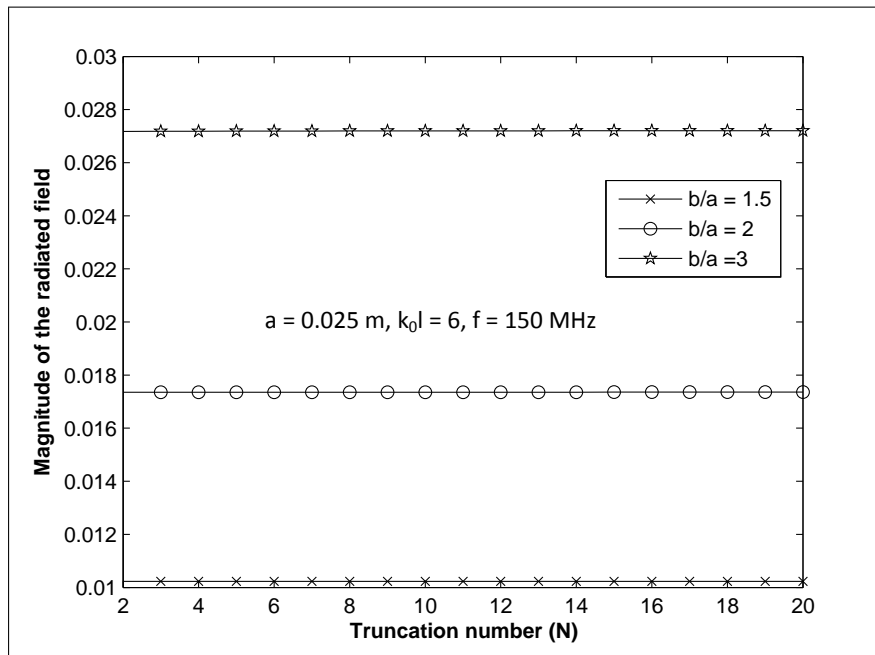


Figure 2.10: Radiated field versus the truncation number  $N$ .



### 3. TEM WAVE RADIATION FROM A DIELECTRIC-FILLED COAXIAL WAVEGUIDE WITH A LARGE CIRCUMFERENTIAL GAP ON ITS OUTER WALL

In this section, as well as a finite slit of length  $l$  on the outer wall, we will assume the interior region of the waveguide ( $a < \rho < b$ ) is characterized by the relative permittivity  $\epsilon_r$  (Figure 3.1). The wave numbers for the regions  $\rho > b$  and  $a < \rho < b$  are denoted by  $k_0 = w\sqrt{\epsilon_0\mu_0}$  and  $k_1 = w\sqrt{\epsilon_1\mu_0}$ , respectively, with  $\epsilon_1 = \epsilon_0\epsilon_r$ .

Similarly to the Section 2, the incident TEM mode propagating in the positive  $z$  direction be given by

$$H_\phi^i(\rho, z) = u_i(\rho, z) = \frac{e^{ik_1z}}{\rho} \quad (3.1)$$

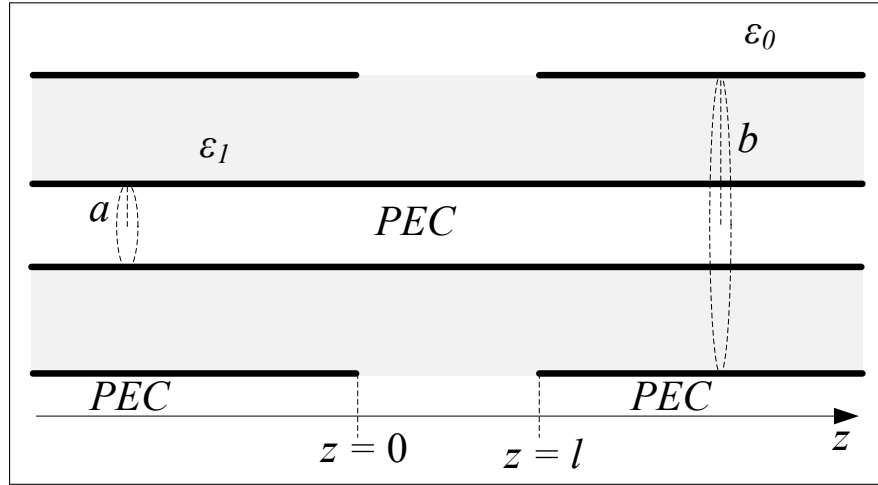


Figure 3.1: Geometry of the problem.

#### 3.1. Formulation of the Problem

Note that, the total electromagnetic field can be expressed as

$$u_T(\rho, z) = \begin{cases} u_i(\rho, z) + u_1(\rho, z), & a < \rho < b \\ u_2(\rho, z), & \rho > b \end{cases} \quad (3.2)$$

where  $u_1(\rho, z)$  and  $u_2(\rho, z)$  are the scattered fields which satisfy the boundary conditions and continuity relations in their relevant regions

$$u_1(a, z) + a \frac{\partial u_1(a, z)}{\partial \rho} = 0, \quad z \in (-\infty, \infty), \quad (3.3)$$

$$u_1(b, z) + b \frac{\partial u_1(b, z)}{\partial \rho} = 0, \quad z \in \{(-\infty, 0) \cup (l, \infty)\}, \quad (3.4)$$

$$u_2(b, z) + b \frac{\partial u_2(b, z)}{\partial \rho} = 0, \quad z \in \{(-\infty, 0) \cup (l, \infty)\}, \quad (3.5)$$

$$\varepsilon_0 \left\{ u_1(b, z) + b \frac{\partial u_1(b, z)}{\partial \rho} \right\} = \varepsilon_1 \left\{ u_2(b, z) + b \frac{\partial u_2(b, z)}{\partial \rho} \right\}, \quad z \in (0, l), \quad (3.6)$$

$$\frac{e^{ik_1 z}}{b} + u_1(b, z) = u_2(b, z), \quad z \in (0, l). \quad (3.7)$$

Additionally, to ensure the uniqueness of the solution, one has to take into account the radiation condition and the edge conditions given in the previous section. In their relevant regions the scattered fields  $u_1(\rho, z)$  and  $u_2(\rho, z)$  satisfy the Helmholtz equations

$$\left[ \frac{\partial^2}{\partial \rho^2} + \frac{1}{\rho} \frac{\partial}{\partial \rho} + \frac{\partial}{\partial z^2} + \left( k_1^2 - \frac{1}{\rho^2} \right) \right] u_1(\rho, z) = 0 \quad (3.8)$$

and

$$\left[ \frac{\partial^2}{\partial \rho^2} + \frac{1}{\rho} \frac{\partial}{\partial \rho} + \frac{\partial}{\partial z^2} + \left( k_0^2 - \frac{1}{\rho^2} \right) \right] u_2(\rho, z) = 0 \quad (3.9)$$

whose Fourier transform yield

$$\left[ \frac{\partial^2}{\partial \rho^2} + \frac{1}{\rho} \frac{\partial}{\partial \rho} + \left( K_1^2(\alpha) - \frac{1}{\rho^2} \right) \right] F(\rho, \alpha) = 0 \quad (3.10)$$

and

$$\left[ \frac{\partial^2}{\partial \rho^2} + \frac{1}{\rho} \frac{\partial}{\partial \rho} + \left( K_0^2(\alpha) - \frac{1}{\rho^2} \right) \right] G(\rho, \alpha) = 0 \quad (3.11)$$

respectively. Here,  $K_0(\alpha) = \sqrt{k_0^2 - \alpha^2}$  and  $K_1(\alpha) = \sqrt{k_1^2 - \alpha^2}$  are the square-root

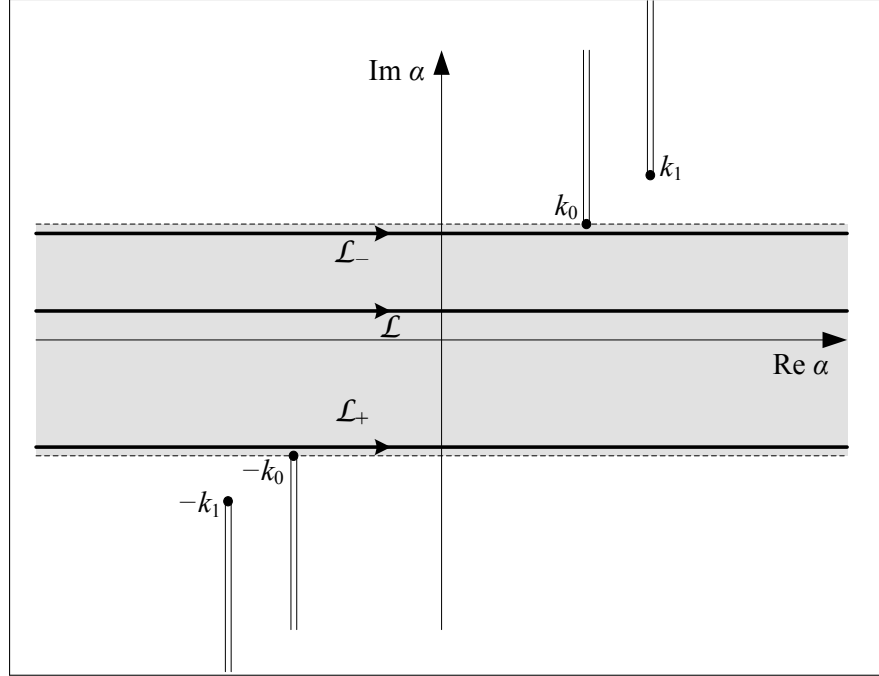


Figure 3.2: Complex  $\alpha$  - plane.

function defined in the complex  $\alpha$  - plane cut along as shown in Figure 3.2, such that  $K_0(0) = k_0$  and  $K_1(0) = k_1$ . As before in the previous section, the general solutions of Eqs. (3.10) and (3.11) yield

$$F(\rho, \alpha) = A(\alpha)J_1(K_1\rho) + B(\alpha)Y_1(K_1\rho), \quad (3.12)$$

and

$$G(\rho, \alpha) = C(\alpha)H_1^{(1)}(K_0\rho). \quad (3.13)$$

respectively. The Fourier transform of the boundary condition (3.3) gives

$$F(a, \alpha) + aF_1'(a, \alpha) = 0, \quad (3.14)$$

which reads

$$B(\alpha) = -A(\alpha) \frac{J_0(K_1 a)}{Y_0(K_1 a)}. \quad (3.15)$$

On the other hand, the Fourier transform of boundary condition (3.4) yields

$$A(\alpha) = \frac{Y_0(K_1 a) [F_1(b, \alpha) + bF_1'(b, \alpha)]}{K_1 b [J_0(K_1 b)Y_0(K_1 a) - J_0(K_1 a)Y_0(K_1 b)]} \quad (3.16)$$

Taking into account these relations, one can write

$$F(\rho, \alpha) = \frac{[F_1(b, \alpha) + bF_1'(b, \alpha)] [J_1(K_1 \rho)Y_0(K_1 a) - J_0(K_1 a)Y_1(K_1 \rho)]}{K_1 b [J_0(K_1 b)Y_0(K_1 a) - J_0(K_1 a)Y_0(K_1 b)]} \quad (3.17)$$

From equations (3.5) and (3.6), we have

$$C(\alpha) = \frac{[G_1(b, \alpha) + bG_1'(b, \alpha)]}{K_0 b H_0^1(K_0 b)} H_1^1(K_0 \rho) \quad (3.18)$$

and

$$\varepsilon_0 [F_1(b, \alpha) + bF_1'(b, \alpha)] = \varepsilon_1 [G_1(b, \alpha) + bG_1'(b, \alpha)] \quad (3.19)$$

Lastly, incorporating ((3.15)-(3.19)) into the continuity relation given by (3.7), one determines the Wiener-Hopf equation

$$\frac{M(\alpha)}{K_0^2(\alpha)b} P_1(\alpha) + P_-(\alpha) + e^{i\alpha l} P_+(\alpha) = \frac{[e^{i(\alpha+k_1)l} - 1]}{ib(\alpha + k_1)} \quad (3.20)$$

with

$$P_1(\alpha) = F_1(b, \alpha) + bF_1'(b, \alpha), \quad (3.21)$$

$$P_+(\alpha) = F_+(b, \alpha) - G_+(b, \alpha), \quad (3.22)$$

$$P_-(\alpha) = F_-(b, \alpha) - G_-(b, \alpha), \quad (3.23)$$

and

$$M(\alpha) = \frac{K_0 \varepsilon_0 H_1^1(K_0 b)}{\varepsilon_1 H_0^1(K_0 b)} - \frac{K_0^2 [J_1(K_1 b) Y_0(K_1 a) - J_0(K_1 a) Y_1(K_1 b)]}{K_1 [J_0(K_1 b) Y_0(K_1 a) - J_0(K_1 a) Y_0(K_1 b)]}. \quad (3.24)$$

Following the procedures described in " Appendices B and C ", one can determine the split functions  $M_+(\alpha)$  and  $M_-(\alpha)$ . By multiplying both sides of (3.20) by  $e^{-i\alpha l}(\alpha + k_0)/M_+(\alpha)$  and  $(k_0 - \alpha)/M_-(\alpha)$ , respectively, we get

$$\begin{aligned} \frac{P_1(\alpha) e^{-i\alpha l} M_-(\alpha)}{b(k_0 - \alpha)} + \frac{P_+(\alpha)(k_0 + \alpha)}{M_+(\alpha)} + \frac{e^{-i\alpha l}(k_0 + \alpha)}{M_+(\alpha)} L(\alpha) \\ = \frac{e^{ik_1 l}(k_0 + \alpha)}{ib(\alpha + k_1) M_+(\alpha)} \end{aligned} \quad (3.25)$$

and

$$\begin{aligned} \frac{P_1(\alpha)}{b(k_0 + \alpha)} M_+(\alpha) + \frac{P_-(\alpha)(k_0 - \alpha)}{M_-(\alpha)} + \frac{e^{i\alpha l}(k_0 - \alpha)}{M_-(\alpha)} U(\alpha) \\ = -\frac{(k_0 - \alpha)}{ibk_1 + \alpha} M_-(\alpha) \end{aligned} \quad (3.26)$$

with

$$U(\alpha) = P_+(\alpha) - \frac{e^{ik_1 l}}{ib(\alpha + k_1)} \quad (3.27)$$

and

$$L(\alpha) = P_-(\alpha) + \frac{e^{ik_1 l}}{ib(\alpha + k_1)}. \quad (3.28)$$

The third term of (3.25) and the third term and the right hand side of the equation (3.26) have singularities in both half-planes. After performing the Wiener-Hopf decomposition procedure and analytical continuation principle, one obtains

$$\frac{(k_0 + \alpha)}{M_+(\alpha)} U(\alpha) = -\frac{1}{2\pi i} \int_{L^+} \frac{e^{-i\tau l} L(\tau)(k_0 + \tau)}{M_+(\tau)(\tau - \alpha)} d\tau \quad (3.29)$$

and

$$\frac{(k_0 - \alpha)}{M_-(\alpha)} L(\alpha) = \frac{1}{2\pi i} \int_{L^-} \frac{e^{i\tau l} U(\tau) (k_0 - \tau)}{M_-(\tau)(\tau - \alpha)} d\tau + \frac{(k_0 + k_1)}{ib(k_1 + \alpha)M_+(k_1)} \quad (3.30)$$

Applying the classical Wiener-Hopf method as in the previous problem, one can obtain the pair of simultaneous integral equations

$$\frac{(k_0 + \alpha)}{M_+(\alpha)} \tilde{U}(\alpha) = \frac{1}{2\pi i} \int_{L^-} \frac{e^{i\tau l} (k_0 - \tau) \tilde{U}(\tau)}{M_-(\tau)(\tau + \alpha)} d\tau + \frac{(k_0 + k_1)}{ib(k_1 - \alpha)M_+(k_1)} \quad (3.31)$$

$$\frac{(k_0 + \alpha)}{M_+(\alpha)} \tilde{L}(\alpha) = -\frac{1}{2\pi i} \int_{L^-} \frac{e^{i\tau l} (k_0 - \tau) \tilde{L}(\tau)}{M_-(\tau)(\tau + \alpha)} d\tau - \frac{(k_0 + k_1)}{ib(k_1 - \alpha)M_+(k_1)} \quad (3.32)$$

where  $\tilde{U}(\alpha)$  and  $\tilde{L}(\alpha)$  are defined by

$$\tilde{U}(\alpha) = U(\alpha) + L(-\alpha) \quad (3.33)$$

$$\tilde{L}(\alpha) = U(\alpha) - L(-\alpha). \quad (3.34)$$

This is the same case as before in the previous problem except with  $k$  replaced by  $k_1$ . Thus we can use the method of successive approximation to solve integral equation system for large  $k_{0,1}l$  and obtain

$$\tilde{U}_1(\alpha) = \frac{(k_0 + k_1)M_+(\alpha)}{ib(k_1 - \alpha)M_+(k_1)(k_0 + \alpha)}, \quad (3.35)$$

$$\tilde{L}_1(\alpha) = -\frac{M_+(\alpha)(k_0 + k_1)}{ib(k_0 + \alpha)(k_1 - \alpha)M_+(k_1)} \quad (3.36)$$

and

$$\tilde{U}_2(\alpha) = \tilde{L}_2(\alpha) = -\frac{(k_0 + k_1)}{2\pi b M_+(k_1)} I_2(\alpha) \quad (3.37)$$

with

$$I_2(\alpha) = \int_{L^-} \frac{e^{i\tau l} M_+(\tau)(k_0 - \tau)}{M_-(\tau)(\tau + \alpha)(k_1 - \tau)(k_0 + \tau)} d\tau \quad (3.38)$$

The above integral is calculated by closing the contour in the upper half plane and evaluating the residue contributions from the simple poles occuring at the zeros of  $M(\alpha)$  lying in the upper half plane as follows

$$I_2(\alpha) = \frac{e^{ik_0 l} M_+^2(k_0)}{2ik_0 \pi b} \beta(a, b, l, k_0, k_1, \alpha) + 2\pi i \sum_{s=1}^{\infty} \frac{e^{i\gamma_s l} (k_0 - \gamma_s) M_+^2(\gamma_s)}{(\gamma_s - \alpha)(k_1 - \gamma_s)(k_0 + \gamma_s) M'(\gamma_s)} \quad (3.39)$$

where  $\gamma'_s$  s are the zeros of  $M(\alpha)$  and

$$\beta(a, b, l, k_0, k_1, \alpha) = \int_0^{\infty} \frac{te^{-tl} \varepsilon_0 \varepsilon_1 4i K_1^2 [J_0(K_1 b) Y_0(K_1 a) - J_0(K_1 a) Y_0(K_1 b)]}{(t - i(k_0 + \alpha))(k_1 - k_0) F(t)} dt \quad (3.40)$$

with

$$F(t) = K_0^2 \{ [J_0(K_1 b) Y_0(K_1 a) - J_0(K_1 a) Y_0(K_1 b)] \times [\varepsilon_0^2 K_1^2 H_1^{(1)}(K_0 b) H_1^{(2)}(K_0 b) + \varepsilon_1^2 K_0^2 H_0^{(1)}(K_0 b) H_0^{(2)}(K_0 b)] \} - 2\varepsilon_0 \varepsilon_1 K_1 K_0^3 \{ [J_1(K_1 b) Y_0(K_1 a) - J_0(K_1 a) Y_1(K_1 b)] \times [J_1(K_0 b) J_0(K_0 b) + Y_0(K_0 b) Y_1(K_0 b)] \} \quad (3.41)$$

to be evaluated numerically. Therefore, one arrives at

$$U(\alpha) = -\frac{M_+(\alpha)(k_0 + k_1)}{(k_0 + \alpha) 2\pi b M_+(k_1)} I_2(\alpha) \quad (3.42)$$

$$L(\alpha) = \frac{M_-(\alpha)(k_0 + k_1)}{ibM_+(k_1)(\alpha + k_1)(k_0 - \alpha)} \quad (3.43)$$

and

$$P_1(\alpha) = -\frac{(k_0 + \alpha)(k_0 + k_1)}{iM_+(k_1)(k_1 + \alpha)M_+(\alpha)} + \frac{(k_0 - \alpha)e^{i\alpha l}(k_0 + k_1)}{2\pi M_+(k_1)M_-(\alpha)} I_1(\alpha). \quad (3.44)$$

### 3.2. Analysis of the Fields

Taking into account equations (3.17), (3.21) and (3.44), the scattered field for the region  $\rho > b, -\infty < z < \infty$  is given by the inverse Fourier transform

$$u_2(\rho, z) = \frac{1}{2\pi} \int_L \frac{\varepsilon_0 P_1(\alpha)}{\varepsilon_1 K_0 b H_0^{(1)}(K_0 b)} H_1^{(1)}(K_0 \rho) e^{-i\alpha z} d\alpha \quad (3.45)$$

Using the asymptotic expansion of  $H_1^{(1)}(K_0 \rho)$  for large arguments as follows

$$H_1^{(1)}(K_0 \rho) \simeq \sqrt{\frac{2}{\pi K_0 \rho}} e^{i(K_0 \rho - 3\pi/4)} \quad (3.46)$$

and applying the saddle point technique yields

$$u_2(r, \theta) = -D(\theta) \frac{e^{ik_0 r}}{k_0 r} \quad (3.47)$$

with



$$\begin{aligned}
D(\theta) = & -\frac{\varepsilon_0(k_0 + k_1)}{\varepsilon_1 \pi b \sin \theta H_0^{(1)}(k_0 b \sin \theta)} \\
& \times \left\{ \frac{-k_0(1 - \cos \theta)}{i(k_1 - k_0 \cos \theta) M_+(-k_0 \cos \theta) M_+(k_1)} \right. \\
& + \frac{(1 + \cos \theta) e^{ik_0 l(1 - \cos \theta)} M_+^2(k_0) \beta(a, b, l, k_0, k_1, -k_0 \cos \theta)}{4i\pi M_+(k_1) M_+(k_0 \cos \theta)} \\
& \left. + \frac{e^{-ik_0 l \cos \theta} i k_0 (1 + \cos \theta)}{M_+(k_0 \cos \theta) M_+(k_1)} \sum_{s=1}^{\infty} \frac{e^{i\gamma_s l} (k_0 - \gamma_s) L(-\gamma_s) M_+^2(\gamma_s)}{M'(\gamma_s) (k_0 + \gamma_s) (k_1 - \gamma_s) (\gamma_s - k_0 \cos \theta)} \right\} \quad (3.48)
\end{aligned}$$

### 3.3. Numerical Results

For the radiated field, some numerical results are obtained and are shown in Figures 3.3-3.8, where the variation of the radiated field pattern, normalized as  $|D(\theta)| / |1/a|$  with respect to the observation angle  $\theta$  is presented for different values of  $b/a$ ,  $\varepsilon_r$ ,  $k_1 l$  and frequency. In these figures, strong radiation is observed in the forward and backward directions along the waveguide walls, due to the directive effect of the outer surface of the waveguide walls for TEM waves. This characteristic is also seen in the case of a circular waveguide with a large gap on its wall, which is studied rigorously in [Elmoazzen and Shafai, 1974].

In order to provide a comparison of the analysis done in this paper with the previous study for hollow coaxial waveguides [Öztürk and Çınar, 2013], the normalized magnitude of the radiated field is presented in Fig. 3.3 for  $\varepsilon_r = 1$ ,  $b/a = 1.5$ ,  $k_1 l = 6$  and  $f = 150$  MHz and an excellent agreement is observed between the Wiener-Hopf analysis with both types of factorization methods and the analysis by the use of simple series representation. However, when the waveguide is filled with a dielectric material, it is observed from Fig. 3.4 that the factorization method matters and the one described in "Appendix C" has a better agreement with the result obtained by simple series method although with a slight difference for smaller observation angles (considering the scale of the vertical axis). Such a difference could be expected as there is less information in the analysis done by simple series method, such as the lack of the use of edge conditions. A similar conclusion is done for the comparison of Wiener-Hopf analysis and mode-matching technique in

[Öztürk and Çınar, 2013] and [Aksimsek et al., 2013]. In Fig. 3.5, the variation of the normalized magnitude of the radiated field with respect to  $b/a$  ratio is illustrated and it is seen that the magnitude is increasing with increasing  $b/a$  ratio. This characteristic was also observed in hollow coaxial waveguides as in [Öztürk and Çınar, 2013]. The effects of the relative permittivity of the dielectric material inside the waveguide and the frequency are presented in Figures. 3.6 and 3.7, respectively. The normalized magnitude of the radiated field is increasing when  $\epsilon_r$  is decreasing or the frequency is increasing. Finally, in Figure 3.8, the variation of the normalized magnitude of the radiated field with respect to  $k_1 l$  is illustrated. As for the hollow coaxial waveguide case in [Öztürk and Çınar, 2013], it is observed that  $k_1 l$  has very little effect on the radiated field.

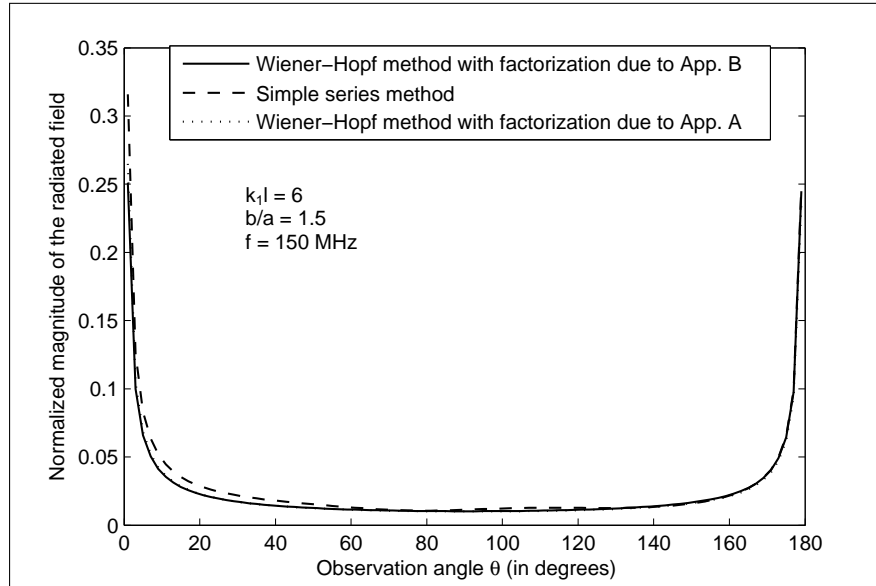


Figure 3.3: Comparison for  $\epsilon_r = 1$ .

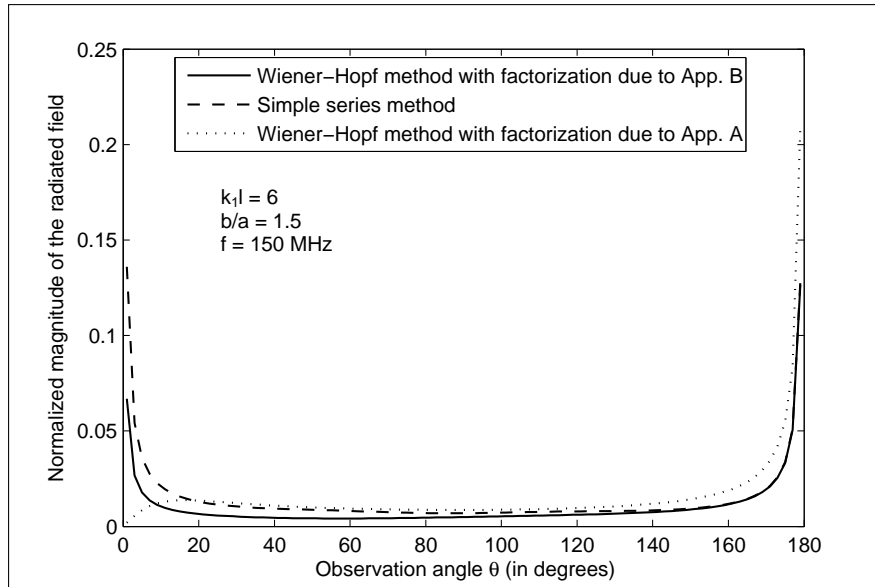


Figure 3.4: Comparison for  $\epsilon_r = 2.4$ .

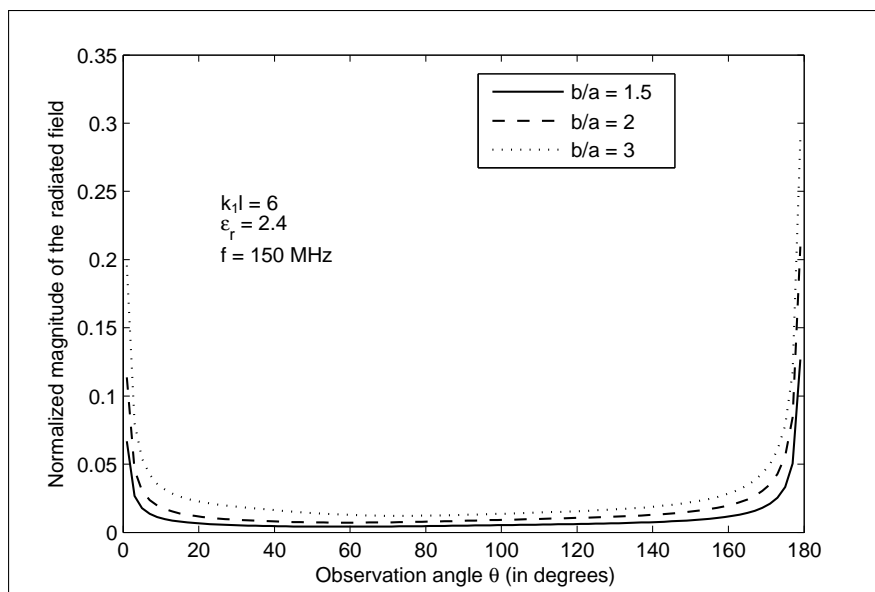


Figure 3.5: Variation of the radiated field with respect to  $b/a$ .

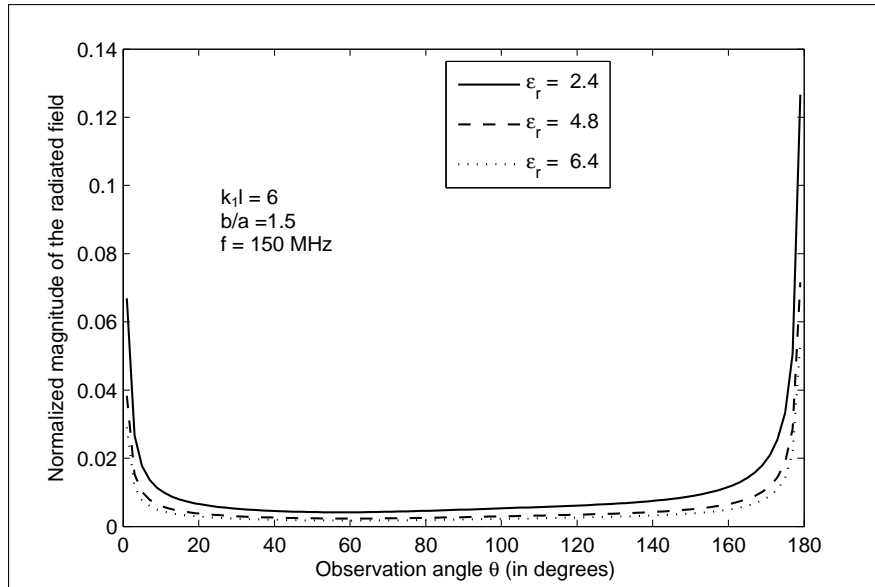


Figure 3.6: Variation of the radiated field with respect to  $\epsilon_r$ .

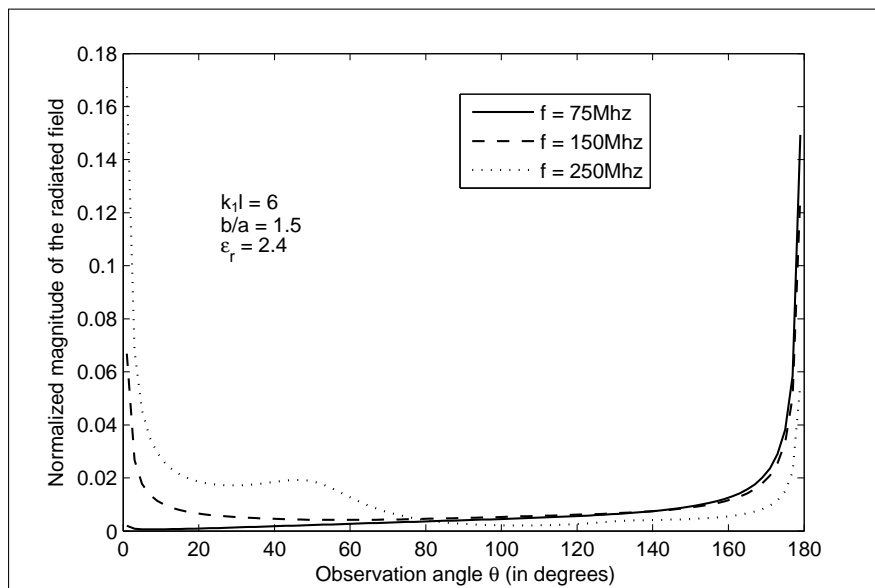


Figure 3.7: Variation of the radiated field with respect to frequency.

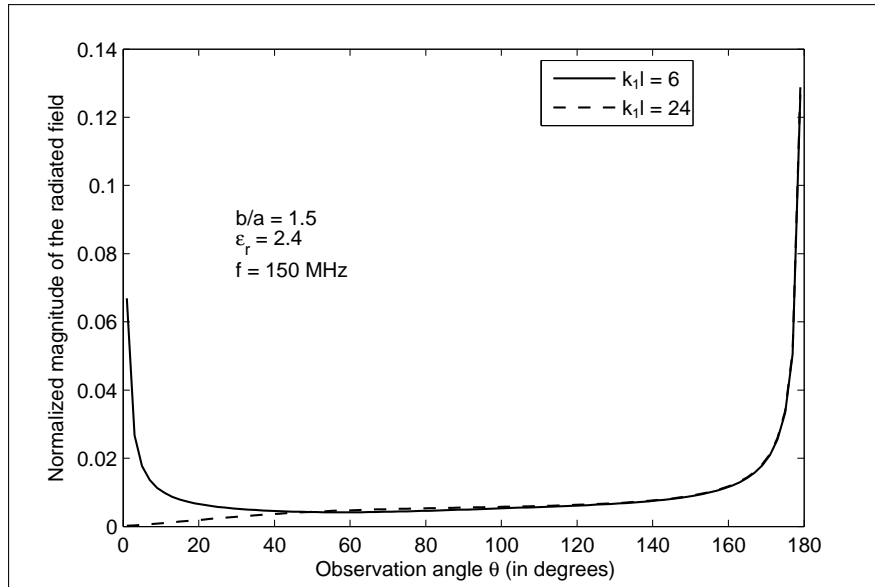


Figure 3.8: Variation of the radiated field with respect to  $k_1 l$ .

## 4. CONCLUDING REMARKS

In this thesis, the TEM wave propagation in an hollow and dielectric-filled coaxial waveguides having a large gap on its outer wall is analyzed rigorously by applying direct Fourier transform which yields a modified Wiener-Hopf equation of the first type. The modified Wiener-Hopf equation is reduced to a Fredholm integral equation of the second type, which is solved iteratively. Finally, the diffraction coefficients related to the reflected, transmitted and radiated fields are determined explicitly for large gap width compared to the wavelength. It is observed that when the waveguide is filled with a dielectric material, the factorization method described in " Appendix B " lacks accuracy, which is an important conclusion for future studies. Besides, the effects of the cross-sectional area of the coaxial cylindrical waveguide, the gap width and the frequency on the radiated field are presented graphically. The behaviour of the radiated field has been observed to be similar to that of in [Elmoazzen and Shafai, 1974] and in [Öztürk and Çınar, 2013] for  $\epsilon_r = 1$ . This analysis can also be applied to the case where the medium outside the waveguide is complex. Also, having coated walls on the waveguide after the gap would also be very interesting problem in the sense of microwave filters.

## REFERENCES

- Aksimsek S., Çınar G., Nilson B., Nordebo S., (2013), “TEM wave scattering by a step discontinuity on the outer wall of a coaxial waveguide”, *IEEE Transactions on Microwave Theory and Techniques*, 61(8), 2783-2791.
- Büyükaksoy A., Çınar G., Serbest A.H., (2004), “Scattering of plane waves by a junction of a transmissive and soft/hard half-planes”, *Zeitschrift fuer Angewandte Mathematik und Physik* , 55(3), 483-499.
- Chang D. C., (1973), “Equivalent circuit representation and characteristics of a radiating cylinder driven through a circumferential slot”, *IEEE Transactions on Antennas and Propagation*, 21(6), 792-796.
- Cho Y. K., (1987), “Analysis of a narrow slit in a parallel-plate transmission line: E polarization case”, *Electronics Letters*, 23(21), 1105-1106.
- Çınar G., Büyükaksoy A., (2004), “Plane wave diffraction by a slit in an impedance plane and a complementary impedance strip”, *Radio Science*, 39(2), 242-251.
- Elmoazzen Y. E., Shafai L., (1973), “Mutual coupling between parallel-plate waveguides ”, *IEEE Transactions on Microwave Theory and Techniques*, 21(12), 825-833.
- Elmoazzen Y. E., Shafai L., (1974), “Mutual coupling between two circular waveguides”, *IEEE Transactions on Antennas and Propagation*, 22(6), 751-760.
- Hurd R. A., (1973), “The field in a narrow circumferential slot in a coaxial waveguide”, *Canadian Journal of Physics*, 51(9), 946-955.
- Kobayashi K., (1993), “Some diffraction problems involving modified Wiener-Hopf geometries”, In: Hashimoto M., Idemen M., Tretyakov O.A., Editors, “Analytical and Numerical Methods in Eletromagnetic Wave Theory”, Science House.
- Lee S. U., Eom H. J., Kwon J. H., (2011), “TEM mode in the GTEM cell”, *Journal of Electromagnetic Waves and Applications* , 25(4), 519-526.
- Melkumyan A., (2007), “On acoustic and electric waves diffraction in piezoelectric medium by a permeable half-plane crack”, *Zeitschrift fuer Angewandte Mathematik und Physik*, 58(2), 330-349.
- Mitra R., Lee S. W., (1971), “Analytical Techniques in the Theory of Guided Waves”, 1st Edition, McMillan.
- Moiola A., Hiptmair R., Perugia I., (2011), “Plane wave approximation of homogeneous Helmholtz solutions ”, *Zeitschrift fuer Angewandte Mathematik und Physik*, 62(5), 809-837.

- Morita N., Nakanishi Y., (1968), "Circumferential gap  $TE_{01}$ -mode transmitting multimode circular waveguide", IEEE Transactions on Microwave Theory and Techniques, 16(3), 183-189.
- Öztürk H., Çınar G., (2013), "Scattering of a TEM wave by a large circumferential gap on a coaxial waveguide ", Journal of Electromagnetic Waves and Applications, 27(5), 615-628.
- Park J. K., Eom H. J., (2000), "Radiation from multiple circumferential slots on a coaxial cable", Microwave and Optical Technology Letters, 26(3), 160-162.
- Park J. K., Eom H. J., (2003), "TM scattering by a gap on a circular waveguide", Microwave and Optical Technology Letters, 37(2), 146-148.
- Polat B., (1999), "Diffraction of acoustic waves by a cylindrical impedance rod of finite length", Zeitschrift für Angewandte Mathematik und Mechanik, 79(8), 555-567.
- Sautbekov S. S., (2011), "Diffraction of plane wave by strip with arbitrary orientation of wave vector", Progress In Electromagnetics Research , 21, 117-131.
- Seran S., Donohoe J. P., Topsakal E., (2009), "Diffraction from a material loaded tandem slit ", IEEE Transactions on Antennas and Propagation, 57(11), 3500-3511.
- Serbest A. H., Büyükaksoy A., (1993), "Diffraction by strips and slits", In: Hashimoto M., Idemen M., Tretyakov O.A., Editors, "Analytical and Numerical Methods in Electromagnetic Wave Theory", Science House.
- Sheingold L. S., Storer J. E., (1954), "Circumferential gap in a circular waveguide excited by a dominant circular-electric wave", Journal of Applied Physics, 25, 545-552.
- Tayyar İ. H., Büyükaksoy A., Işıkyer A., (2008), "Wiener-Hopf analysis of the parallel-plate waveguide with finite length impedance loading", Radio Science, 43(5), 114-125.
- Wait J. R., Hill D. A., (1975a), "On the electromagnetic field of a dielectric coated coaxial cable with an interrupted shield", IEEE Transactions on Antennas and Propagation, 23(4), 470-479.
- Wait J. R., Hill D. A., (1975b), "Electromagnetic fields of adielectric coated coaxial cable with an interrupted shield-quasi-static approach", IEEE Transactions on Antennas and Propagation, 23(5), 679-682.



## **BIOGRAPHY**

Hülya ÖZTÜRK was born in İstanbul, Turkey, in 1984. She got a Bsc degree in Department of Mathematics from Gebze Institute of Technology, in 2008. She received a M.Sc degree in Mathematics from Gebze Institute of Technology, in 2010. She has been working as a research assistant at Gebze Technical University, since 2009.

# APPENDICES

## Appendix A: Publications Based on the Thesis

Öztürk H., Çınar G., (2013), “Scattering of a TEM wave by a large circumferential gap on a coaxial waveguide”, *Journal of Electromagnetic Waves and Applications*, 27(5), 615-628.

Öztürk H., Çınar G., Yanaz Çınar Ö., (2014), “TEM wave radiation from a dielectric-filled coaxial waveguide with a large circumferential gap on its outer wall”, *Zeitschrift fuer Angewandte Mathematik und Physik*, DOI: 10.1007/s00033-014-0445-2.

Öztürk H., Çınar G., (2012), “TEM wave radiation from an aperture on a coaxial waveguide”, *Days on Diffraction*, St. Petersburg, Russia, 28 May - 1 June.

Öztürk H., Çınar G., Yanaz Çınar Ö., (2013), “Radiation characteristics of a dielectric-filled circular waveguide with a large circumferential gap”, *International Conference on Applied Analysis and Mathematical Modeling*, Istanbul, Turkey, 2-5 June.

## Appendix B: Factorization of $M(\alpha)$ with the first procedure

In order to solve the Wiener-Hopf equation (3.20), one must first factorize the kernel function  $M(\alpha)$  as follows

$$M(\alpha) = M_+(\alpha) M_-(\alpha) \quad (\text{B1.1})$$

which can be done by following the procedures described in [Seran et al., 2009] as follows

$$M_+(\alpha) = M_-(-\alpha) = \sqrt{M(0)} e^{A_+(\alpha)-s} \quad (\text{B1.2})$$

with

$$A_+(\alpha) = \frac{1}{2\pi i} \int_{L^+} \frac{\ln[M(t)]}{t - \alpha} dt \quad (\text{B1.3})$$

and

$$s = \frac{1}{2\pi i} \int_{L^+} \frac{\ln[M(t)]}{t} dt \quad (\text{B1.4})$$

Above, the integration contour for  $A_+(\alpha)$  and  $s$  can be modified as follows

$$A_+(\alpha) = \frac{1}{2\pi i} \int_{k'_1 - i\eta}^{\infty - i\eta} \frac{\ln[M(t)]}{t^2 - \alpha^2} 2\alpha dt + \frac{1}{2\pi i} \int_C \frac{\ln[M(t)]}{t - \alpha} dt \quad (\text{B1.5})$$

and

$$s = \frac{1}{2\pi i} \int_C \frac{\ln[M(t)]}{t} dt. \quad (\text{B1.6})$$

respectively, with  $k'_1$  being the real part of  $k_1$ . The integration path can be seen in Figure B1.1.

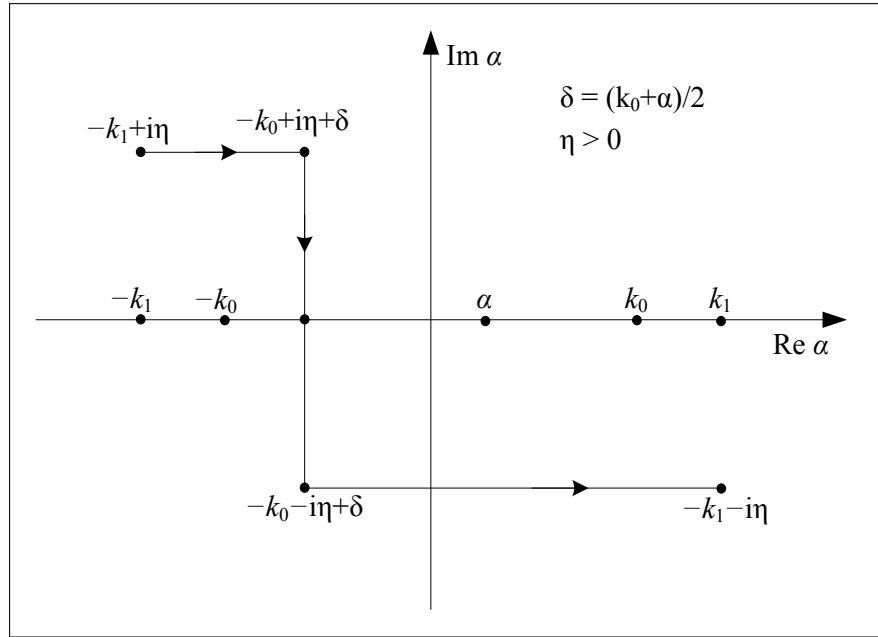


Figure B1.1: Path of integration.

## Appendix C: Factorization of $M(\alpha)$ with the second procedure

New formal expressions for the split functions  $M_+(\alpha)$  and  $M_-(\alpha)$ , satisfying  $M(\alpha) = M_+(\alpha) M_-(\alpha)$  can also be derived by the following procedure described in [Mittra and Lee, 1971] defining

$$M_1(\alpha) = \varepsilon_1 K_1^2 [J_0(K_1 b) Y_0(K_1 a) - J_0(K_1 a) Y_0(K_1 b)], \quad (\text{C1.1})$$

$$\begin{aligned} M_2(\alpha) &= \frac{1}{H_0^{(1)}(K_0 b)} \\ &\times \left\{ \varepsilon_0 K_0 K_1^2 H_1^{(1)}(K_0 b) [J_0(K_1 b) Y_0(K_1 a) - J_0(K_1 a) Y_0(K_1 b)] \right. \\ &\quad \left. - \varepsilon_1 K_1 K_0^2 H_0^{(1)}(K_0 b) [J_1(K_1 b) Y_0(K_1 a) - J_0(K_1 a) Y_1(K_1 b)] \right\} \end{aligned} \quad (\text{C1.2})$$

and

$$M_+(\alpha) = M_-(\alpha) = \frac{M_{2+}(\alpha)}{M_{1+}(\alpha)} \quad (\text{C1.3})$$

to give

$$\begin{aligned} M_{1+}(\alpha) &= \sqrt{\varepsilon_1} (k_1 + \alpha) \sqrt{J_0(k_1 b) Y_0(k_1 a) - J_0(k_1 a) Y_0(k_1 b)} \\ &\times \prod_{m=1}^{\infty} (1 + \alpha/\alpha_m) e^{i\alpha(b-a)/m\pi} \\ &\times \exp \left\{ \frac{\alpha}{\pi i} (b-a) \left[ 1 - C + \log \left( \frac{2\pi i}{k_1 (b-a)} \right) \right] \right\} \end{aligned} \quad (\text{C1.4})$$

with  $\alpha'_m$  s being the zeros of  $J_0(k_1 b) Y_0(k_1 a) - J_0(k_1 a) Y_0(k_1 b)$  and

$$\begin{aligned}
M_{2+}(\alpha) &= \sqrt{M_2(0)} \prod_{m=1}^{\infty} (1 + \alpha/\gamma_m) \\
&\times \exp \left[ -\frac{ik_0(a-b)}{2} + \frac{K_0(\alpha)(a-b)}{\pi} \log \left( \frac{\alpha + iK_0(\alpha)}{k_0} \right) \right] \\
&\times \exp [q(\alpha)]
\end{aligned} \tag{C1.5}$$

with  $C = 0.57721\dots$ ,  $\gamma'_m$  s being the zeros of  $M_2(\alpha)$  and

$$q(\alpha) = P \int_0^{\infty} \left[ \frac{(a-b)}{\pi} - \frac{\{B(w) + B(we^{i\pi})\}}{2\pi i} \right] \log \left( 1 + \frac{\alpha}{[k_0^2 - w^2]^{1/2}} \right) dw \tag{C1.6}$$

In the above expressions,  $P$  notation denotes the Cauchy principle value at the singularity  $w = k_0$  and  $B(w)$  can be written as follows

$$\begin{aligned}
B(w) &= \frac{1}{\tilde{B}(w)} \{ A_1(w) C_1(w) + A_2(w) C_2(w) \\
&\quad - \varepsilon_1 \left[ H_0^{(1)}(wb) \right]^2 w^3 a A_3(w) \\
&\quad + \left( \varepsilon_0 \tilde{w} w^2 a H_1^{(1)}(wb) H_0^{(1)}(wb) \right) A_4(w) \}
\end{aligned} \tag{C1.7}$$

with

$$\begin{aligned}
\tilde{B}(w) &= H_0^{(1)}(wb) \left\{ \varepsilon_0 w \tilde{w}^2 H_1^{(1)}(wb) \left[ J_0(\tilde{w}b) Y_0(\tilde{w}a) - J_0(\tilde{w}a) Y_0(\tilde{w}b) \right] \right. \\
&\quad \left. - \varepsilon_1 \tilde{w} w^2 H_0^{(1)}(wb) \left[ J_1(\tilde{w}b) Y_0(\tilde{w}a) - J_0(\tilde{w}a) Y_1(\tilde{w}b) \right] \right\}, \tag{C1.8}
\end{aligned}$$

$$A_1(w) = \left[ J_0(\tilde{w}b) Y_0(\tilde{w}a) - J_0(\tilde{w}a) Y_0(\tilde{w}b) \right], \tag{C1.9}$$

$$A_2(w) = \left[ J_1(\tilde{w}b) Y_0(\tilde{w}a) - J_0(\tilde{w}a) Y_1(\tilde{w}b) \right], \tag{C1.10}$$

$$A_3(w) = \left[ J_1(\tilde{w}a) Y_1(\tilde{w}b) - J_1(\tilde{w}b) Y_1(\tilde{w}a) \right], \quad (\text{C1.11})$$

$$A_4(w) = \left[ J_1(\tilde{w}a) Y_0(\tilde{w}b) - J_0(\tilde{w}b) Y_1(\tilde{w}a) \right], \quad (\text{C1.12})$$

$$\begin{aligned} C_1(w) = & \varepsilon_1 H_1^{(1)}(wb) H_0^{(1)}(wb) 2w^2 \\ & + \varepsilon_0 w \tilde{w}^2 b \left[ \left( H_0^{(1)}(wb) \right)^2 + \left( H_1^{(1)}(wb) \right)^2 \right] \\ & - \varepsilon_1 \left( H_0^{(1)}(wb) \right)^3 w^3 b, \end{aligned} \quad (\text{C1.13})$$

$$C_2(w) = -\varepsilon_0 H_1^{(1)}(wb) H_0^{(1)}(wb) w^2 \tilde{w} b - \varepsilon_1 \left( H_0^{(1)}(wb) \right)^2 2\tilde{w} w, \quad (\text{C1.14})$$

and

$$\tilde{w} = \sqrt{w^2 + k_1^2 - k_0^2}. \quad (\text{C1.15})$$

## Appendix D: Convergence of the $\beta(a, b, l; \alpha)$

Let's split the integral in a sum of two terms:

$$\begin{aligned} \beta(a, b, l; \alpha) = & \int_0^1 \frac{e^{-tl}}{[t - i(k + \alpha)]} \frac{[J_0(Kb) Y_0(Ka) - J_0(Ka) Y_0(Kb)]^2}{J_0^2(Ka) + Y_0^2(Ka)} dt \\ & + \int_1^\infty \frac{e^{-tl}}{[t - i(k + \alpha)]} \frac{[J_0(Kb) Y_0(Ka) - J_0(Ka) Y_0(Kb)]^2}{J_0^2(Ka) + Y_0^2(Ka)} dt \end{aligned} \quad (\text{D1.1})$$

Since the integrand is continuous for  $t \in [0, 1]$ , the first integral is convergent. For the second integral, by utilizing the following asymptotic expansions as  $t \rightarrow \infty$ ,

$$[J_0(Kb) Y_0(Ka) - J_0(Ka) Y_0(Kb)]^2 \simeq \frac{4}{\pi^2 t^2 ab} \sin^2(t(a - b)), \quad (\text{D1.2})$$

$$J_0^2(Ka) + Y_0^2(Ka) \simeq \frac{2}{\pi ta} \quad (\text{D1.3})$$

it is appropriate to use limit comparison test with  $g(t) = \frac{2e^{-tl}}{\pi bt^{3/2}} \sin^2(t(a-b))$ , which is continuous except 0. For  $t > 1$  holds

$$\left| \frac{2e^{-tl}}{\pi bt^{3/2}} \sin^2(t(a-b)) \right| \leq \frac{1}{t^{3/2}}. \quad (\text{D1.4})$$

Since  $\int_1^{\infty} \frac{1}{t^{3/2}} dt$  converges,  $\int_1^{\infty} \frac{2e^{-tl}}{\pi bt^{3/2}} \sin^2(t(a-b)) dt$  is absolutely convergent. Moreover,

$$\lim_{t \rightarrow \infty} \left| \frac{\frac{e^{-tl}}{[t-i(k+\alpha)]} \frac{[J_0(Kb)Y_0(Ka) - J_0(Ka)Y_0(Kb)]^2}{J_0^2(Ka) + Y_0^2(Ka)}}{\frac{2e^{-tl}}{\pi bt^{3/2}} \sin^2(t(a-b))} \right| = 0. \quad (\text{D1.5})$$

Since  $\int_1^{\infty} \frac{2e^{-tl}}{\pi bt^{3/2}} \sin^2(t(a-b)) dt$  is absolutely convergent, we conclude that  $\int_1^{\infty} \frac{e^{-tl}}{[t-i(k+\alpha)]} \frac{[J_0(Kb)Y_0(Ka) - J_0(Ka)Y_0(Kb)]^2}{J_0^2(Ka) + Y_0^2(Ka)} dt$  is convergent. Therefore, the improper integral  $\beta(a, b, l; \alpha)$  is convergent.